Late Pleistocene-Holocene palaeoenvironmental evolution of the Añamaza River valley (Iberian Range, NE Spain): multidisciplinary approach on the study of carbonate fluvial systems.

A. Luzón [a], *, A. Gauthier [b], A. Pérez [a], O. Pueyo-Anchuela [a], M.J. Mayayo [a], A. Muñoz [a]

[a] Departamento de Ciencias de la Tierra, Facultad de Ciencias, Universdad de Zaragoza, Pedro Cerbuna 12, 50009 Zaragoza, Spain

[b] Laboratoire de G eographie Physique: Environnements Quaternaires et Actuels, CNRS UMR 8591 LGP e Universit es Paris 1 & UPEC/Paris 12, CNRS Meudon, 1, place Aristide Briand, 92195 Meudon, Cédex, France

Abstract

The uppermost Pleistocene and Holocene palaeoenvironmental evolution of the Añamaza river valley (Iberian Range, NE Spain) is deduced using multidisciplinary approach including stratigraphical, mineralogical, palynological, geochemical, geophysical methods and drilling. Main changes were registered in distinct subenvironments of a carbonate fluvial system, including the channelled zone and wetlands in the floodplain.

Tufa barrages dominated although pools also existed. Geophysical survey and coring reveal tufa build-ups and pool facies also in the subsoil. Lower water temperature and scarce evaporation are deduced for the Pleistocene fluvial system that progressively changed through the Holocene, with more hydrologically closed areas and higher evaporation influence. A general aggrading evolution during warm stages related with increasing base level and damming due to fast carbonate precipitation, characterised the Holocene. Detrital tufa indicates erosive high-energy floods or colder stages when water level would decrease favouring erosion. ^{14}C and $^{230}Th/^{234}U$ dating reveal high sedimentation rates and three main discontinuities related with cold episodes: Younger Dryas, middle part of the Holocene Climate Optimum and Iron Age Epoch. During the uppermost Pleistocene tufa growth would be enhanced during warmer episodes as the Bølling/Allerød. In the Younger Dryas scarce vegetation favoured erosion of both, slopes and tufa constructions. Subsequent warmer temperatures during the first part of the Holocene favoured vegetated slopes, enhanced tufa growing (although interrupted in the middle part of the Holocene Climate Optimum), and development of wetlands with riparian vegetation in the floodplain, where either siliciclastics or detrital tufa incoming alternated with low-energy waters stages and mud settling. Progressive decline in tufa is deduced for the upper Holocene but it is not possible to determine whether this, and other palaeoenvironmental changes were related either to climate or increasing human activities. During the Roman and Medieval Warm Periods more oxidizing conditions in the wetlands and increasing erosion prevailed, probably conditioned by human activities.

The pollen record shows for the Early Holocene development of Pinus forest with Betula, and expansion of deciduous Quercus, xerophilous and heliophilous grassland. Subsequent increasing moisture supported open forests with deciduous (Quercus, Ulmus, Corylus) and

evergreen (Quercus ilex, Pistacia) species. From ca.4000 yrBP, a dominant deciduous Quercus forest with groves of Corylus, Ulmus, Acer, Fagus and Taxus expanded and human activities (grazing) occurred. From 1200 yrBP dry grassland expanded due to intensive land use (agro-pastoral activities). Almost completely deforested plateaus surround the site today with slopes covered by patchy grass with junipers groves and screeds with little soil.

1. Introduction

Ancient fresh water carbonate fluvial systems have been profusely studied all around the world mainly by analysing their most common and best preserved deposits: fluvial tufa constructions. A common topic on fluvial tufa systems studies has been sedimentology, with the main aim to recognize and interpret lithofacies and lithofacies associations and to propose coherent sedimentological models (Ordóñez and García del Cura, 1983; Pedley; 1990; 2009; Ford and Pedley, 1996; Zamarreño et al., 1997; Martín Algarra et al., 2003; Ordóñez et al., 2005; Carthew et al, 2006; Vázquez Úrbez et al., 2010, Arenas et al., 2014; García-García et al., 2014). In fluvial systems fitting with the barrage/pool model (Pedley, 1990; 2009; Ford and Pedley, 1996), other kind of deposits mostly generated in the fluvial floodplains (e.g. detrital tufa and muds) are rarely studied due to their scarce preservation potential: they are highly erodible facies intensely exposed to erosion during common entrenchment stages (Ordóñez et al., 2005; Ortiz et al., 2009). Climate has been traditionally considered the main control factor on active tufa generation, which is favoured during warm and wet episodes (Pedley et al., 1996; Andreo et al., 1999; Horvatinčić et al., 2000; Zak et al., 2002; Martín Algarra et al., 2003; Pedley, 2009; Sancho et al.; 2015). Nevertheless, tufas also develop in other climate regimes (Willing, 1985; Pedley, 2009). Moreover, water level fall stages associated fluvial downcutting or destructive floods, cause often erosion of previous sediments (Vaudour, 1986; Taylor et al., 1994; Carthew et al., 2003; Ordóñez et al., 2005) and for this reason identification of sedimentary hiatuses in the series can be of equal importance on the study of palaeoenvironmental changes.

In any case, carbonate fluvial systems dynamics is not only climate-dependent and it is widely known that can be controlled by other factors, both natural or antrophic (Goudie et al., 1993; Bell and Walker, 1992; Pentecost and Viles, 1994; Viles and Pentecost, 2007; Capezzuoli et al., 2014), which can strongly complicate the knowledgement of the system and avoid correct palaeoenvironmental interpretations to be attained. For these reasons, during the last years, new research fields highlight the great importance of fluvial carbonates not only on the study of climate (Andrews et al., 1997; 2000; Kano et al., 2004; Andrews and Brasier, 2005; Capezzuoli et al., 2010; Luzón et al., 2011) but also of hydrological changes (Golubić, 1969; Kano et al., 2007; Auqué et al., 2013), tectonic setting (Sbeinati et al.; 2010; Pazzaglia et al., 2013; Ascione et al., 2014; Henchiri, 2014; Camuera et al., 2015) or anthropogenic influence (Goudie et al., 1993; Limondin-Lozouet et al., 2010) in the area where this kind of facies have developed. For the moment, most of the studied fluvial tufas are Quaternary in age as, commonly, only fragmentary erosional remnants of the fluvial system preserve (Pedley, 2009; Capezzuoli et al., 2014). In this sense, the study of fluvial carbonate systems has benefited greatly during the last years of the use of coring methods (Pedley et al., 1996; 2000; Ordóñez et al., 2005; Sbeinati et al.; 2010) or shallow geophysical techniques that allow to better define internal geometries and not outcropping sectors to be studied (Pedley et al., 2000; Pedley and Hill, 2003; Pérez et al., 2012).

The present work is focused on the study of non-outcropping deposits belonging to a carbonate fluvial system developed during the Late Pleistocene-Holocene in the central Iberian Range (Spain), and the interpretation of the main palaeoenvironmental changes occurred in the area. Tufas in the channelled area have been considered, but also detrital tufas and mud deposits in the floodplain. The innovative aspect is that a multidisciplinary approach including stratigraphical, palynological, geophysical, geochemical and mineralogical studies all together has been followed on the study of different parts of the system, which difficult, but reinforce, palaeoenvironmental interpretations as they fit with all the considered proxies and have been registered in different parts of the system.

2. Geological setting

The Añamaza River valley is located in the central area of the Iberian Range (Fig. 1). The geological succession in the region is mainly Mesozoic (Middle Jurassic-Lower Cretaceous) and Tertiary in age. The Mesozoic is represented by the carbonate Chelva Formation (Middle Jurassic), the terrigenous Tera Group (Jurassic-Cretaceous transition) and the carbonate Oncala Group (Cretaceous). Conglomerates, lutites and limestones integrate the Tertiary series, which lies subhorizontal and unconformably on the Mesozoic rocks. Winter temperatures in the region are low (December and January mean temperatures below 4°C) and summers relatively warm (August mean temperature 19.9°C). The average annual rainfall is about 600 mm although there is significant inter-annual variability. During the summer months, the subtropical Azores anticyclone blocks moisture transport from the west. The vegetation dominant species in the heights are *Quercus ilex* and *Quercus rotundifolia* as well as *Quercus faginea* and *Quercus canariensis*, whereas at lower altitude *Erica spp*, *Juniperus spp, Poaceae* and *Thero-Brachypodietea* predominate.

The studied fluvial deposits form part of a Late Pleistocene-Holocene complex sedimentary system (Luzón et al., 2011) integrated by alluvial fans, passing downstream to a shallow lake (Añavieja Lake). Lacustrine deposits are represented by black and brown muds related to settling and carbonate precipitation. Both, alluvial fans and lake were located upstream the area where this study is focused. Downstream the lake, several stepped tufa barrages separated small lakes or natural pools, ore slow flowing areas (Sáenz and Sanz, 1989; Coloma et al., 1996; Pérez et al., 2010; Luzón et al.; 2011; Arenas et al., 2014). The sedimentary system had a catchment area of about 140 km^2 and water supplies included superficial discharges, but mainly groundwater (Coloma et al., 1996). Groundwater supplies to the Añamaza River come from the Jurassic aquifer; in fact, conductivity values (600-900 μS/cm) and bicarbonate-sulphate calcium composition of this aquifer show clear similarity with the Añamaza River water. On the contrary, groundwater in the Quaternary aquifer has a predominantly sulphate calcium composition and higher conductivity values (1000-1400 μS/cm). Springs mainly concentrate in two zones: i) close to Añavieja village, at 960 m.a.s.l. (Fig. 1) supplying a flow of 160 l/s, and ii) close Dévanos village, at 950 m.a.s.l., with 40 l/s (Coloma et al., 1996). Tufa deposits in the area are considered to have formed discontinuously from the Miocene to the Holocene. Arenas et al. (2014) proposed a detailed lithofacies classification for the Pleistocene and Holocene tufas and two different fluvial models related respectively to moderate and high slope reaches of the valley. The moderate-slope model that these authors consider representative for the Holocene, included extensive standing-water areas dammed by barrage-cascades; the high-slope model, consisted of small slow flowing areas between cascades and barrage-cascades. The Holocene tufas are located slightly higher than the present course of the river (Luzón et al., 2011; Auqué et al., 2013; Arenas et al., 2014).

3. Methodology

Different methods have been used for the study of the Añamaza fluvial carbonate deposits, in order to test and compare the potential of distinct sediments as palaeoenvironmental registers. As previously indicated, sedimentary facies analysis was the focus of previous works by Luzón et al. (2011) and Arenas et al. (2014); the latter made a facies analysis based on outcropping deposits and the former also considered data from cores. For this reason, lithofacies descriptions are not included in the present work.

3.1. Coring

Three new cores were drilled by rotation in the system with an RL-48-L device. They were named AÑ1.2, DV2 and DV3 (Fig. 1), which have, respectively, the following UTM coordinates: 30TWM856462, 30TWM883404, and 30TWM882406. AÑ1.2 (15.5 m-long) was drilled mainly for palynological study, in a wide flat area located between two ancient tufa barrages, close to the previously extracted AÑ1 (Luzón et al., 2011; 2012) and the valley wall. DV2 (16.8-long) was drilled over a tufa barrage, and DV3 (21 m-long) immediately upstream it, in a zone interbarrages. The extracted cores were kept in humid conditions (more than 95% humidity) until being studied. In the Laboratory of Stratigraphy of the Zaragoza University, they were carefully split and photographed and their study was carried out following the protocol recommended by the Limnological Research Centre (Schnurrenberger et al., 2003). Description of each core included lithology, colour, texture, micro and macroscopic biological content, and sedimentary structures.

3.2. Chronology

The chronology of AÑ1.2 core was established by AMS (accelerator mass spectrometry) ^{14}C dating on six samples. Selection of the samples was conditioned by the presence of organic material trying to avoid potential “hard water effect” problems. Necessary preparation and samples pre-treatment for radiocarbon dating was carried out by the ^{14}C Laboratory of the

Department of Geography at the University of Zurich (GIUZ). The dating itself was done by AMS with the tandem accelerator of the Institute of Particle Physics at the Swiss Federal Institute of Technology in Zurich (ETH). ^{14}C ages were calibrated using IntCal program (Reimer et al., 2009). Five samples from the dominantly carbonate DV2 core were dated using Uranium-series disintegration method (Ivanovich and Harmon, 1992) at Geochronology Laboratory of the ICT Jaume Almera (Barcelona, Spain). The chemical separation of the radioisotopes and purification followed the procedure described by Bischoff et al. (1988). The isotope electrodeposition was carried out using the method described by Talvitie (1972), modified by Hallstadius (1984). The separated isotopes were counted in an Alpha Ortec Octete Plus spectrometer and age calculations were based on the computer program of Rosenbauer (1991).

3.3. Mineralogical analysis

The mineralogical composition of seventy-two samples from AÑ1.2 was determined on the whole sample by X-ray diffraction (XRD) using a Philips PW 1710 diffractometer with Cu-K α radiation, automatic divergence slit and graphite monochromator, belonging to the Zaragoza University. The XRD data were stored as computer files with the XPowder software (Martín, 2004). To compare the study samples, an estimation of whole-sample mineral abundance was carried out using the normalized reference intensity ratio method (Chung, 1974; Jenkins and Snyder, 1996) and the weighting factors of Schultz (1964). The error of the semiquantitative determination is about 5%.

3.4. Isotopical analysis

Twenty-six calcite isotopic analyses ($\delta^{18}O_{Cc}$ and $\delta^{13}C_{Cc}$) on bulk sample were performed at the Stable Isotopes Laboratory of the Salamanca University. Samples, 10-15 mg, were leached with 1 ml 100% pure H_3PO_4, at 25ºC under vacuum conditions (McCrea, 1950). The resulting CO_2 was extracted following the techniques described by Walters et al. (1972). The analyses were carried out in a SIRA II mass spectrometer. The precision of the method is 0.2‰ for $\delta^{18}O$ and 0.1‰ for $\delta^{13}C$. The isotope data are presented relative to the international VPDB standard (Craig, 1957; Gonfiantini, 1984).

3.5. Pollen analysis

A total of fifty-six samples were taken at 30 cm intervals for pollen analysis from the AÑ1.2 core, except at the lower part in which the intervals were of 8-10 cm. At least 350 pollen grains (minimum of 100 pollen grains apart from the most dominant taxa) and 20 different taxa were identified and counted per sample. Pollen percentages were calculated on a basic pollen sum that excluded aquatic plants (Cyperaceae, *Alisma*, *Callitriche*, *Cladium*, *Myriophyllum alterniflorum*-t., *Myriophyllum verticillatum*-t., *Hydrocharis morus-ranae*, Lythraceae, *Menyanthes*, *Nymphaea*, *Polygonum amphibium*-t., *Potamogeton*, *Sparganium-Typha*-t., *Typha latifolia*), Pteridophytes spores, indeterminables, unknowns and Algae. Aquatic plants percentages were calculated from the main pollen sum (basic sum plus Aquatic plants). Pteridophytes spores, indeterminables and unknown percentages were calculated from the main pollen sum plus Pteridophytes spores, indeterminables and unknowns. Algae were added to this total sum to calculate their percentages. The calculation of pollen concentrations followed the volumetric method of Cour (1974). The pollen diagrams were constructed using Psimpoll program (Bennett, http://www.chrono.qub.ac.uk/psimpoll/psimpoll.html). Samples of 1.5 g of sediment were prepared using standard palynological procedures (Faegri and Iversen, 1989). After physical (sieving through 160 μm mesh screens) and chemical (HF, HCl, KOH and acetolysis) treatment, pollen residues were diluted in glycerol and 40 μl were mounted on slides. Pollen and spores were identified and counted at a magnification of ×500 (oil immersion) and ×1000 (oil immersion). Pollen determination was performed with pollen keys and pollen atlases (Moore et al., 1991; Beug, 2004; Reille, 1992; 1995; 1998), and using the reference collection of the Laboratoire de Géographie Physique (LGP) of CNRS-Université Paris 1-UPEC. Distinctions within the Poaceae are based on the classification depending on size and morphological features (Faegri and Iversen, 1989; Moore et al., 1991; Beug, 2004). Four groups were differentiated: Poaceae (wild grass pollen grains), *Hordeum*-t., *Secale*-t. and *Triticum*-t. (including *Triticum* and *Avena* pollen grains). Differentiation of three pollen types within *Quercus* pollen is based on specific morphological keys from Planchais (1962), Colombo et al. (1983) and van Benthem et al. (1984). Pinus stomata types were identified using identification keys of Trautmann (1953), Hansen (1995), Sweeney (2004) and García Álvarez et al. (2009a, 2009b).

3.6. Geophysical survey

Ground Penetrating Radar (GPR) survey was carried out along different zones were barrages and pools were expected to be present in the subsoil (Fig. 1) avoiding the presence of sharp topographical changes. 120 GPR profiles parallel and normal to the current flow river direction were made, comprising more than 8300 meters of linear survey. The use of different antennas allows us attain different resolution and research depths. In general, high frequency antennas give high resolution but low penetration while low frequency ones give higher depth but less resolution. A preliminary analysis through different antennas was performed to constrain the most appropriate ones to be later systematically used; 100 and 250 MHz antennas were finally selected (41 profiles using 100 MHz and 42 profiles using 250 MHz). GPR wave propagation velocity was established by the modelling of diffraction hyperbolae at profiles and comparison with DV2 and DV3 boreholes. This analysis permitted us to constrain a propagation velocity ranging from 78 to 113 m/μs with a mean value of 90 m/μs for the whole area. Propagation velocity is in the range of the obtained in similar settings (Annan, 1992; Dagallier et al., 2000; Kruse et al., 2000; Pedley and Hill, 2003 Neal, 2004; Mukherjee et al., 2010; McBride et al., 2012). After surveying, a similar data processing was applied to each profile: through time-zero correction, filter of frequencies out of range, running average or stacking to avoid irregular surficial displacement (in order to avoid significant resolution looses during processing, each trigger was defined for 1024 samples and trig distance established over the horizontal resolution). Exponential and linear gain was used to intensify GPR waves at middle to high depths, in some cases until GPR wave saturation, and in others to constrain significant reflectors in the subsoil. Background removal and subtract mean trace procedures were also applied for erasing the subhorizontal distribution of GPR-records due to the sinusoidal wave characteristics.

4. Results

The location of the extracted cores inside the system and their lithological features allow them to be analysed from different perspectives, all enabling a more complete knowledge of the palaeoenvironmental evolution. AÑ1.2 core, drilled on fine terrigenous facies with macrophyte organic remains and some sand-size detrital tufas, preserves valuable pollen information. Mainly carbonate DV2 and DV3 cores have been more useful on the GPR study, because, on the contrary to AÑ1.2 sediments, which avoid waves penetration, they are made of highly reflective materials.

4.1 Chronology

AÑ1.2 ^{14}C dating indicates a Holocene age for these deposits (Table 1 and Fig. 2). Datings are in the range of those obtained by Luzón et al. (2011) in the AÑ1 core, drilled few metres to the East (Luzón et al., 2012), also included in Table 1. $^{230}Th/^{234}U$ datings on DV2 support a Late Pleistocene-middle Holocene age for these deposits (Table 2 and Fig. 3) and reveal a possible sedimentary hiatus between metres 15 and 16. These dating suggest the 16.5 uppermost metres of the DV2 core to represent a similar age that the sediments between ca. 8 and 12 m depth in AÑ1.2. It is worth nothing that the Late Pleistocene materials on this DV2 are harder as a consequence of higher cementation.

4.2 Wetlands in the floodplain: AÑ1.2 core

4.2.1 Lithological characterization

Six lithological units can be distinguished in AÑ1.2 core (Fig. 3). The lowest (U1) is the most terrigenous one, integrated by siliceous and carbonate gravels and interbedded sands and silts. The second unit (U2) is made of black and brown muds alternating with intraclastic tufa beds. In Unit 3 (U3) silts and muds are interbedded with macrophyte remains and intraclastic tufa. Unit 4 (U4) is made of alternating black muds and macrophyte remains with some silty intercalations; intraclastic tufa is nearly absent. Unit 5 (U5) shows less macrophyte remains and Unit 6 (U6) is made of brown and black bioturbated muds. Dominant dark muds with macrophyte organic remains and intraclastic tufa in AÑ1.2 indicate a commonly flooded vegetated area contiguous to the main channelled zone. Episodes of incoming terrigenous supplies (siliciclastic sand and tufa debris) alternated with stages of more stagnant waters and mud settling; terrigenous facies are more common in the lower part. Intraclastic tufa is related to the erosion of tufa build-ups (e.g. barrages or small phytoherms) located upstream, and occurred especially during deposition of U2 and U3, in the lower part of the Holocene.

Mean mineralogical composition for each unit (Table 3) shows that the average quartz content is the highest in U1, decreases towards U5 and subsequently increases again in U6.

Phyllosilicate mean increases, in general, from base to top, although slightly decreases in U5. Calcite mean shows a reverse trend to quartz, increasing in a general manner from U1 to U5, and clearly decreasing in U6. The average pyrite content is low and almost constant from U1 to U4, very low on U5, and it is not present in U6. Mean values of gypsum are low in all the differentiated units. The general decrease in quartz towards the, could be related to increasing vegetation cover in the surrounding mountain areas; nevertheless siliciclastics increase (phyllosilicates and quartz) is inferred again for U6. Calcite in U1 to U4 is related to the existence of intraclastic tufa and carbonate silts, whereas this kind of sediments are not visible with the naked eye in U5 and 6, suggesting carbonate precipitation. The high organic matter content and the existence of pyrite is related to the prevalence of anoxic and acidic conditions in the sediment, almost temporarily, avoiding the complete mineralisation of the organic matter (Luzón et al., 2011) and perhaps mire conditions, especially in relation U1 to U4.

4.1.2 Pollen analysis results

Two pollen diagrams are presented. In the pollen percentages diagram on figure 3, some selected pollen and spore data are presented; a complete pollen diagram with all taxa can be found in the Supplementary file. The summary pollen diagram (Fig. 4) includes taxa diversity, pollen concentration curve and groups established on the basis of the ecological requirements and/or as anthropogenic indicators of the corresponding plants. Nine local pollen zones have been defined based on variations of the relative frequencies of both natural and anthropogenic pollen, according on the definition by Gordon and Birks (1972). A brief description of the local pollen zones is presented in Table 4. Throughout most of the pollen record, pollen concentrations greatly fluctuate ranging from 242666 to 8317 grains/g, highlighting, as lithofacies do, an irregular sedimentation with alternating periods of significant deposition and phases of stop in sedimentation. The highest values characterize the first part of the pollen record (pollen zones Ana-1 to Ana-4) and from pollen zone Ana-5 upward, pollen concentrations gradually decrease.

The first pollen zone Ana-1 is dominated by *Pinus*. Other taxa such as *Juniperus*, *Betula* and deciduous *Quercus* developed. Herbaceous pollen taxa such as Poaceae, Asteroideae, Cichorioideae as well as steppic plants (*Ephedra distachya*, *Artemisia* and Chenopodiceae) show significant values. The pollen zone Ana-2 is characterized by high *Pinus* values, the increase of thermophilous taxa such as deciduous *Quercus*, *Corylus*, *Ulmus* and of Mediterranean taxa, mainly *Quercus ilex*, while a marked decrease in *Juniperus*, *Betula*, *Artemisia* and Asteroideae percentages is recorded. These last taxa increase again in pollen zone Ana-3. Ana-4 is characterized by high *Pinus* values, the development of deciduous *Quercus*, *Corylus* and *Quercus ilex*. The decrease in steppic plants and pioneers trees values correspond to the development of Poaceae, Cyperaceae and Monoletes spores.

A major change occurs in pollen zone Ana-5, as attested by the marked decrease in *Pinus* percentages and the simultaneous expansion of deciduous trees and Mediterranean taxa. A diverse assemblage of trees develops: deciduous *Quercus*, *Corylus*, *Taxus*, *Ulmus*, *Hedera*, *Acer* and *Fagus* are recorded. Poaceae and Cyperaceae show increasing frequencies. Anthropogenic indicators and *Cerealia* display a continuous curve. The pollen zone Ana-6 is characterized by a decrease of *Pinus* and deciduous trees while Mediterraean taxa remain stable. The pollen zone Ana-7 indicates increasing values of Poaceae, anthropogenic indicators (mainly *Plantago lanceolata*), Cyperaceae and *Sparganium-Typha*. Deciduous trees and Mediterranean taxa show stable values while *Pinus* displays gradual decrease. Pollen data from the pollen zone Ana-8 indicate the decline of deciduous trees while a rise in herb pollen is recorded with a maximum of *Cerealia*. In pollen zone Ana-9, the amount of Poaceae reaches its maximum. All the main arboreal taxa decrease or are no longer recorded, except *Juniperus* showing increasing percentages.

4.1.2.1. Reconstruction of vegetation at the Añamaza river valley

Ana-1 (1504-1430 cm): *Dry grassland with pioneer tree open woodland (Juniperus, Betula, Pinus)*

A dry grassland, mainly composed by Poaceae, *Artemisia* and Chenopodiaceae may have been locally present. The increased values of *Juniperus* and *Betula*, associated with the presence of *Pinus* stomata and *Pinus* pollen aggregates suggest the local development of a pioneer tree open woodland (*Pinus*, *Juniperus* and *Betula*). However, long distance pollen transport from lower altitudes may have contributed to the high values of *Pinus*. Isolated deciduous *Quercus*-t. could be present in the area or open *Quercus* forest occurred at lower altitudes.

Ana-2 (1430-1346 cm): *Open temperate and humid forest & development of some Mediterranean plants*

The increased percentages of deciduous *Quercus*-t. and *Corylus* are associated with the continuous presence of deciduous trees such as *Viburnum*, *Ulmus*, *Taxus* and *Hedera*. In parallel, Mediterranean taxa (mainly *Quercus ilex*-t. and other taxa such as *Pistacia*, *Quercus suber*-t. and *Cistus*) show a slight increase. Concomitantly, frequency of pioneer trees (*Betula* and *Juniperus*), steppic taxa (*Artemisia* and Chenopodiaceae-t.) and herbaceous taxa, such as *Helianthemum*, Asteroideae-t. and Cichorioideae-t. decline. The significant values of deciduous trees suggest the local expansion of deciduous groves either in the riparian vegetation or within the always-present *Pinus* forest, as attested by stomata and aggregates of *Pinus*. Sclerophyllous Mediterranean woodlands may have occupied the lowlands. The increasing and diversifying aquatic herbaceous taxa indicate the development of the shore water zone vegetation.

Ana-3 (1346-1295 cm): *Dry grassland with open woodland (Juniperus, Pinus, Quercus)*

Increase in percentages and concentrations of *Artemisia*, Chenopodiaceae-t., *Ephedra*, Asteroideae-t., Cichorioideae-t., *Helianthemum* and Poaceae as well as *Pinus*, *Betula* and *Juniperus* suggests a re-expansion of the dry grassland with an open woodland with *Juniperus*, *Pinus* and *Quercus*. Moreover, the lowland sclerophyllous woodland was reduced as indicated by a decrease of *Quercus ilex*-t., and the absence of *Pistacia* and *Quercus suber*-t.

Ana-4 (1295-1115 cm): *Pinus-Quercus open woodland & Mediterranean plants development*

Pollen data indicate the decline of the dry grassland while increasing in deciduous *Quercus*-t. and *Corylus* percentages is recorded. However, values remain relatively low, suggesting some open deciduous *Quercus* woodlands within *Pinus* forest. Besides, increasing Mediterranean plants (mainly *Quercus ilex*-t. and *Quercus suber*-t.) frequencies suggests a sclerophyllous Mediterranean woodland expansion at lower altitudes. The development of Cyperaceae and Pteridophytes associated with other aquatic herbaceous taxa indicates a marshland vegetation spread on the riparian zone; *Potamogeton* and *Mougeotia* algae records suggest a slow flow.

Ana-5 (1115-710 cm): *Mixed oak forest (Corylus, Ulmus, Taxus, Fagus) with Pinus & Expansion of sclerophyllous Mediterranean woodland (Quercus ilex, Q. suber, Pistacia, Fraxinus ornus, Cistus)*

A major change occurs in this pollen zone suggesting a hiatus in the sedimentary record. This stratigraphic discontinuity is supported by ^{14}C dating and occurred between *ca* 8500 and *ca* 4000 yrBP. Pollen assemblages are characterized in this zone by a simultaneous expansion of deciduous *Quercus*-t. and trees such as *Corylus*, *Ulmus*, *Taxus* and *Fagus*. A diversified *Quercus* woodland developed at the expense of *Pinus* forest. Increasing Mediterranean plants (mainly *Quercus ilex*-t, *Pistacia*, *Quercus suber*-t.) suggest the presence of sclerophyllous woodlands at lower altitudes. Riparian vegetation is well developed and diversified, pointing to more stable conditions on the banks; it includes marshland, dominated by aquatic taxa (mainly Cyperaceae) associated with herbaceous plants such as Apiaceae, Lamiaceae, Liliaceae, Ranunculaceae, *Filipendula*, Rubiaceae and Pteridophytes, and riparian woodland with *Salix*, Apiaceae, *Acer*, *Hedera* and *Populus*. Increased *Plantago lanceolata*-t. and *Rumex* values combined with the presence of *Cerealia*-t. pollen suggest a limited human impact with grazing and crop cultivation activities in the surrounding area.

Ana-6 (710-575 cm): *Open mixed oak forest with riparian meadow and pasture & Sclerophyllous Mediterranean woodland*

An opening of the mixed *Quercus* woodland is inferred from the decreased percentages of deciduous *Quercus*-t, *Taxus* and *Pinus*. This coincides with the development of grazing activities suggested by the increased *Plantago lanceolata*-t., *Rumex* and Poaceae values (percentages and concentrations) and the expansion of the riparian vegetation, in which aquatic plants (Cyperaceae, *Callitriche*, *Myriophyllum*, *Potamogeton* and *Sparganium-Typha*-t.), tall herbaceous (such as Apiaceae, Cichorioideae-t., Lamiceae, Onagraceae, Ranunculaceae, *Sanguisorba minor* and Valerianaceae) and trees (such as *Alnus*, *Salix* and *Fraxinus excelsior*-t.) may constitute a dense wetland vegetation. At lower altitudes, the previously sclerophyllous Mediterranean woodlands are thought to remain stable.

Ana-7 (575-395 cm): *Open mixed oak forest with heath, grassland, important pasture and cereal cultivation & Sclerophyllous Mediterranean woodland*

During this time period *Fagus* become established in the mixed oak forest vegetation, while *Pinus* decline. The increasing percentages of Ericaceae may indicate the development of heath in the understory of *Quercus* woodland. Moreover, in the riparian zone the decrease of *Alnus* and tall herbaceous taxa suggests that the dense wetland vegetation has been replaced by marshland vegetation with Cyperaceae, *Sparganium-Typha*-t. and Pteridophytes. This change in the vegetation around the site is possibly fire-related, as indicated by the simultaneous rise of Ericaceae and *Artemisia* and may be of anthropogenic origin, as indicated by the increased values of Poaceae, *Hordeum*-t. and pollen anthropogenic indicators such as *Plantago*, *Plantago lanceolata*-t. and *Polygonum aviculare*-t., which are associated with grazing (Behre, 1981).

Ana-8 (395-95 cm): *Open mixed oak forest with heath, dry grassland and important cereal cultivation & Sclerophyllous Mediterranean woodland*

The decline of deciduous *Quercus* woodland may be related to human impact from the increasing agricultural practices in the site area, *Cerealia*-t. pollen reaching over 6% at the end of Ana-8 pollen zone. Moreover, parallel with increasing *Juniperus* and *Cistus* values, herbaceous plants such as Poaceae, *Artemisia*, Cichorioideae, Brassicaceae, *Helianthemum*, Crassulaceae and Fabaceae develop. This suggests an expansion of dry grasslands and meadows, recolonizing abandoned pasture lands. In the riparian zone, streamside woodlands composed by *Hedera*, *Acer*, *Populus*, *Salix*, *Alnus* and *Fraxinus excelsior* are present while *Sparganium-Typha* and Pteridophytes are replaced by hygrophilous herbaceous taxa such as *Callitriche*, *Menyanthes*, *Nymphaea* and *Potamogeton*. At lower altitudes, sclerophyllous Mediterranean woodlands (mainly *Quercus ilex*-t., *Quercus suber*-t. and *Pistacia*) are still developed.

Ana-9 (95-10 cm): *Dry grassland with Juniperus*

A significant change is recorded at the end of the sedimentary record. An opening of the landscape and a local loss of woody taxa illustrate an ecological degradation. The decline of the open oak woodlands lead to an expansion of meadows and grasslands with *Juniperus* and xerophilous herbs such as *Artemisia*, Chenopodiaceae-t., Cichorioideae-t., Crassulaceae and *Herniaria*. The disappearance of aquatic herbaceous taxa, such as *Menyanthes*, *Nymphaea* and *Potamogeton* may be indicative of an increased distance from the river shore to the coring site.

4.2 Barrage and pool areas in the channel area: DV2 and DV3 cores

4.2.1 Lithological characterization and dating

Cores DV2 and DV3 (Fig. 5) mainly comprise encrusted tufa with interbedded i) grey marls, ii) brown muds, both including oncolites and intraclastic tufa, and iii) ochre sands. Encrusted beds, 10-20 cm-thick, correspond to phytoherms of either bryophytes or stems, being the latter less common; stromatolites are rarely present. Difference between both cores is mainly related to the lithology of the intercalated non-encrusted beds. In DV2 decametric to metric mud and marl beds with oncolites and intraclastic or phytoclastic tufas (forming wackestone, packstone, floastone and rudstone textures) are recognised. In DV3 yellowish sands are common in the lower part and grey marls in the upper part, both forming decimetre-thick (sometimes up 1 m-thick) beds; marls can include disperse tufa remains as well as oncolites.

Three units have been distinguished for both cores. Unit A1, strongly cemented, is made of phytoherms of stems and phytoclastic tufa (rudstone) related to the destruction of tufa build-ups; some interbedded silts with disperse tufa intraclasts also exist. In Unit A2 the phytoherms alternate with beds made of oncolites and tufa intraclasts; in DV3 core, this unit includes coarser terrigenous facies. Unit A3 supposes a decrease on intraclastic tufas. Oncolites and small phytoherms (both, of stems and bryophytes) are the dominant tufa facies in DV2, whereas in DV3 marls are quite common. Phytoherms in DV2 represent barrage constructions whereas oncolites are interpreted as generated in water-flowing areas, the same that intraclastic tufas, which generated by episodic tufa barrage erosion. DV3, also includes carbonate bioconstructions (smaller than those in DV2) and intraclastic tufas; its general evolution and higher detrital fraction, fits well with a progressive fill of a pool or slow flowing area between barrages. A general reduction in detrital supplies concomitant with the expansion of pool areas over the main barrage constructions can be interpreted for the Holocene.

4.2.2 Isotopical composition

The isotopical composition of the analysed tufas agrees with other Spanish tufas (Pedley, 2009; Andrews et al., 2000; Arenas et al., 2000; García-García et al., 2014). Values are in the range of those obtained in the same area by Arenas et al. (2014), although some values of the Holocene facies are higher than the obtained by them. $\delta^{18}O$ and $\delta^{13}C$ values are shown in Table 5 and figures 5 and 6. For the Late Pleistocene samples (Unit A1) $\delta^{18}O$ and $\delta^{13}C$ vary from -7.39 to -8.52‰ (-7,71 mean value) and from -4.77 to -5.68‰ (-5,23 mean value) respectively. In general $\delta^{18}O$ values are higher in the Holocene samples and the lower $\delta^{13}C$ values are, in general, in Unit A3. Values for the Holocene deposits (A2+A3) vary from -6.34 to -8.12‰ for the $\delta^{18}O$ (-7.06 mean value) and from -4.45 to -7.04‰ for the ^{13}C (-5.43 mean value). Whether the two Holocene units (A2 and A3) are considered separately, in A2 $\delta^{18}O$ values are comprised between -6.34 and -7.24‰, and $\delta^{13}C$ ones between -4.45 and -5.84‰, whereas in the upper unit (A3) $\delta^{18}O$ and $\delta^{13}C$ values are comprised between -6.34 and -8.12‰, and between -5.17 and -7.04‰ respectively. $\delta^{18}O$ and $\delta^{13}C$ mean values are -6.92 and -5.01‰ respectively for A2, and -7.27 and -6.00‰ for A3. $\delta^{18}O$ and $\delta^{13}C$ covariance (Fig. 6) is very poor for the Pleistocene facies with r=0,03, and increases for the Holocene with r=0.74. Considering A2 and A3 separately covariance is better for the upper one (r=0.87) than for the lower one (r=0.43).

4.2.3 Geophysical survey

GPR profiles show a relative good penetration along the studied zone, with similar penetration depth (around 6 to 8 meters) for the different antennas, and common non-horizontal reflectors. In general the records show a structured and reflective media in the upper part (with changing

GPR-refraction style towards deeper zones) overlying a second, noisy media, with no clear reflectors (Fig. 7). The contact between both media is identified with independence of the central frequency of antenna used. The boundary between these two different geophysical media can be tentatively correlated with the boundary between the Holocene tufa deposits and the Mesozoic carbonate rocks. This is supported by: i) Mesozoic rocks outcrop close to the surveyed zones all along the valley, and ii) the contact between the Holocene system and the Mesozoic rocks can be located near the surface or identified in outcrops.

With respect the tufa system, the majority of the profiles exhibit a general reflective behaviour with high contrast and clearly defined reflectors. Nevertheless, some areas are quite different (Fig. 8A), with two main different behaviours (or radarfacies in the sense of Baker, 1991) alternating in the flow direction. These radarfacies have been named A and B (RA and RB hereinafter). Discrimination between RA and RB is easier whit higher frequency antennas. RA corresponds to non-homogeneous reflective areas with hyperbolic anomalies, low to middle propagation velocity, high penetration depth and reflectors with changing dip and random pattern. They resemble the tufa units described as “bright zones” by Pedley et al. (2000). RB corresponds to non-reflective areas with more homogeneous geophysical behaviour, higher propagation velocity and attenuation, as well as subhorizontal reflectors. RB fits better with the results obtained for pool sapropels and silt-muds by Pedley et al. (2000). The physical behaviour and geometrical features of RA and RB (Fig. 8A) allow them to be tentatively correlated with non-outcropping tufa barrages and low-slope or pool media respectively. DV2 and DV3 boreholes, drilled over RA and RB respectively, permit us contrast this interpretation.

The lateral relationship between RA and RB can be also analysed. In figure 8A, RA can be identified in the SE and NW edges, with an intermediate RB sector. Where both facies are in contact, RB is over RA. Lateral relations between RA and RB show an asymmetrical pattern, being related each other by either net subvertical contacts, as occurs in the SE, or by progressive lateral adaptation (in the NW). This overlapping can be identified by the progressive displacement of RB towards the North, drawing onlap geometries. The analysis of the same transect for high frequency antennas (Fig. 8B) allows us to constrain a similar type of contact between RA and RB for the most surficial interval, with a nearly subvertical contact in the southern part of the profile and a more stepped one in the northern part. In these profiles the internal structure of RA shows a distinctive style and reflectivity differences between RA and RB are clearer. Moreover, some hyperbolic anomalies and apparent RA facies can be identified along the central zone where RB dominates that had not been clearly identified in the profiles made with low frequency antennas. These permit us to infer that although the intermediate area shows a RB behaviour it is locally interrupted by RA media, either isolated or laterally connected with other RA in the edges. In the same way, RA in the edges also includes locally RB facies, probably representing detrital facies related to erosion of the carbonate build-ups. The general overlapping of RB over RA can be interpreted as an increase of wideness of the pools (more expansive with time). Lateral changes slightly vary for different TWT-depth intervals (Fig. 9). RA facies located in zones where RB has not been recognised include very different geophysical behaviours.

5. Discussion

5.1. Palaeoenvironmental evolution in the Añamaza valley during the Holocene

The exposed data evince different palaeoenvironmental changes during the Holocene in this area that have been registered in the distinct sedimentary facies and subenvironments. In this sense, our results highlight multidisciplinary approaches, although complicated, as very interesting for geological studies.

Marginal wetland areas in the floodplain are represented by AÑ1.2 core, from which a high sedimentation rate is deduced, as occurs in other parts of the system (Luzón et al., 2011) for the Holocene period. The sedimentary units defined, together with mineralogical and pollen results reveal changes in sedimentation, vegetation and water level in the floodplain through the Holocene. Anoxic conditions were frequent, especially during U1 to U4 deposition, favouring organic matter conservation, including pollen that is a primary source of information about palaeoenvironmental changes in the valley. U1 represents the onset of the Holocene and the high terrigenous content suggests scarcely vegetated areas related to arid conditions, with the gravels in the lower part probably representing the Younger Dryas; this cold stage has been also recognised in nearby zones (Luzón et al.; 2007; Oliva-Urcía et al., 2012, 2016) where it is represented by an increase on coarse detrital supplies. Mineralogical data fit with sedimentological features with a high quartz mean for unit U1. The pollen record also agrees with these interpretations allowing more detailed palaeoenvironmental history to be reconstructed. Considering ^{14}C dating, in the lower part typical characteristics of the early Holocene are recognised. The woodland migration linked to postglacial climatic amelioration starts with a pioneer tree open woodland (*Pinus, Betula* and *Juniperus*) development in a dry grassland (Ana-1), followed from ca 9600 cal BP (Ana-2 - Ana-4) by the establishment of a *Pinus*-*Quercus* open temperate and humid forest (with *Ulmus*, *Corylus* and *Taxus*) and at lower altitudes by sclerophylus Mediterranean woodland (*Quercus ilex*, *Quercus suber* and *Pistacia*) expansion. The dominance of *Pinus* in the vegetation and the progressive replacement of *Pinus* by *Quercus* and other deciduous trees during the early Holocene is a pattern also observed in several regional pollen records (Peñalba, 1994; García Antón et al., 1995; Sánchez Goñi and Hannon, 1999; Gil García et al., 2002; Gil García and Ruiz Zapata, 2004). The increasing and diversifying aquatic herbaceous taxa from An-2 indicate shore water zone vegetation development. In this sense, climate ameloriation favoured the disappearance of xerophilous and heliophilous vegetation and the expansion of wetland vegetation, suggesting increasing water table and slow flowing waters in this site, which fits with tufa widespread. The *Pinus*-*Quercus* open forest expansion is interrupted by a re-expansion of dry grassland (Ana-3); this fluctuation could reveal changes in humidity and suggests a dry climatic event that could be related to those recorded in the Central Ebro Basin (Davis et al., 2007), in the northern Iberian Range (Gil

García et al., 2002) and in other Iberian Peninsula regions (Leira and Santos, 2002; Burjachs et al., 2016; Iriarte-Chiapusso et al., 2016).

Unit U2 (dominated by dark muds and intraclastic tufa) suggests a frequently flooded area where terrigenous were trailed down by flowing waters. Coarse terrigenous (typical in U1) are substituted by intraclastic tufa, probably in relation with tufa growing in the valley and common erosion of non-cemented deposits (e.g. barrages or small phytoherms) located upstream during high energy runoff episodes; these episodes alternated with others of low water energy and mud settling. As wetter and warmer conditions favour the development of tufas (Ford and Pedley, 1996; Sancho et al., 1997; Martín Algarra et al., 2003; Pérez-Obiol et al., 2011; Pla-Pueyo et al., 2015; 2016), the widespread growth of these facies is considered to have been related to the climate amelioration during the first part of the Holocene (Peñalba et al., 1997; Giralt et al., 1999; Gil García et al., 2002; Luzón et al., 2007; Bastida et al., 2013). Such climate conditions would favoured more vegetated slopes, installation of riparian vegetation in the floodplains, slow water flow and a decrease in coarse terrigenous supplies from the source areas, as recognised under warm and more humid conditions in other zones (Faust et al., 2004; Fenech, 2007; Giessner, 1990; Sancho et al., 2008; White et al., 1996; Rohdenburg, 1989; Vásquez-Méndez et al., 2010).

Pollen data, supported with ^{14}C dating, reveal a stratigraphic discontinuity between Ana-4 and Ana-5 zones (middle part of sedimentary unit U2). No sedimentological change has been detected, although the limit between these zones coincides with a change in calcite and siliciclastics vertical trend. The discontinuity would be related to drier conditions, as deduced for the same period in other areas of the Iberian Peninsula (Davis, 1994; Jalut et al., 1997; Giralt et al., 1999; Luzón et al., 2007; 2011) with decreasing water levels and concomitant erosion. From ca. 6000 cal yr BP, a mixed oak forest (with *Corylus, Ulmus, Taxus, Fagus* and *Pinus*) expands and limited human activities (grazing and crop cultivation) are recorded. Riparian vegetation is well developed and diversified, pointing to more stable conditions on the banks and dense wetland vegetation coinciding with the upper part of U2 and lower U3, in which macrophyte organic remains are very common. A significant change in vegetation and local deforestation due to grazing activities is recorded from Ana-6 pollen zone (upper U3). The increase of muds and macrophyte organic remains are related to these environmental changes. Tufa debris reduction from U3 indicates either a decreasing tufa growing or the effect of more stable banks avoiding intraclasts to reach the AÑ1.2 site in the floodplain. In fact, the youngest tufa deposits dated in the area (DV2 core, are ca 4000 yr BP). During U4 deposition (Ana-7 pollen zone) marshland vegetation replaced dense wetlands due to anthropogenic activities (important pasture and cereal cultivation), which perhaps destroyed tufa build-ups. Unit 5 (mainly Ana-8 pollen zone), implies reduced terrigenous supplies suggesting a more humid environment, in agreement with the increase of *Botryococcus* and *Pediastrum* algae and the presence of hygrophilous herbaceous taxa in the riparian zone; in any case a change towards more humid conditions has not been inferred from the rest of vegetation. The intensive land use pattern persisted until the end of the pollen record (Ana-9) marked by dry grasslands expansion with some *Juniperus* groves. Although wet conditions are still maintained in AÑ1.2 site, the disappearance of arboreal cover in the basin favoured again the incoming of terrigenous supplies. The disappearance of aquatic herbaceous taxa during Ana-9 pollen zone (Unit 6) may be indicative of an increased distance from the river shore to the coring site.

Gypsum and pyrite, especially from U1 to U4, is indicative of the existence of sulphate-reducing bacteria working on anoxic conditions, which are typical from saturated wetlands and suggest high water levels and mire conditions, almost during some stages. As no tufa intraclasts exist in the upper units, calcite would be related to palustrine precipitation (Luzón et al.; 2011), implying a more oxidizing and less acidic environment.

Apart from the palaeoenvironmental evolution information, the Añavieja sequence, due to the geographical location of the site in the transitional area between the central Iberian Range and the eastern Ebro Basin, brings new data about the past distribution of cork oak and yew during the Holocene. In NE Spain, the present-day distribution of *Quercus suber* (cork oak) and *Taxus* (yew) shows many separated small areas. Around the study site, isolated small stands of *Quercus suber* are present in Sierra de la Virgen and several pockets of *Taxus* are located in Peña Isasa (Blanco Castro et al., 2005) (Fig. 10) that strongly suggests a larger, more continuous range in the past. The studied pollen record displays two well-differentiated *Quercus suber* and *Taxus* pollen curves (maximum values around 7%) and provides evidence for an early Holocene presence of *Quercus suber* and *Taxus* in the central Ebro Basin since ca 9650 cal yr BP. *Quercus suber* variations correlate well with the other Mediterranean taxa while *Taxus* pollen curve is paralleled by the deciduous *Quercus*-t. pollen curve.

5.2. Stratigraphical arquitecture and isotopical composition: new insights for the dynamics and evolution of the fluvial system

Cores and GPR profiles evince the existence of barrages and pool areas in the subsoil. Lithological and geometrical features allow a better approach to the system configuration through definition of radarfacies. As observed in the scarce outcrops, tufa barrages show more complex internal architecture than pool areas, which are characterised by more tabular beds. Cores, as well as geometries inferred from GPR, have permitted us interpret RA (reflective and non-homogeneous) as tufa constructions and RB (non-reflective and homogeneous) as pool facies. Comparison of DV2 and DV3 cores, and radarfacies, indicates that differences between radarfacies are related to the different architecture and the texture of the detrital beds. RA corresponds to more disorganized areas in which marls with oncolites and intraclastic tufa are common between the tufa phytoherms, whereas the homogeneous behaviour of RB correlates with the existence of carbonate beds with fine terrigenous intercalations.

In more detail, RA facies commonly includes different geophysical behaviours with lateral interruptions of reflectors and very variable dips. They have been interpreted as facies heterogeneities inside the main barrages areas. Laterally related channels filled with oncolites, carbonate clasts or detrital tufa, small phytoherms, bryophytes covering steps in the bottom of the river or stem accumulations have been observed in the outcrops (Luzón et al., 2011; Arenas et al., 2014) and are thought to produce these geometries in RA (Pueyo-Anchuela et al., 2016). Smaller RA zones inside RB also exist that can show continuity with the barrage located downstream, indicating expansion of the barrage, or appear as isolated pockets, suggesting that tufa beds could also developed in the pools, either as small build-ups or barrage erosion products (intraclastic tufa accumulations). Vertical alternation between RB and RA is related to changes in the water depth with time.

RB architecture reflects a geometry dependent of the available space and pool sediments in the upper part of the succession onlapping barrages. They also evince an aggrading system characterized by general adaptation of RB over RA, and anisotropic growth if pools are considered. In this sense, transition between RA and RB is different if downstream or upstream direction is considered (Fig. 8B). In the surveyed zone contacts are more progressive in the downstream face of the barrages, indicating that RB onlaps that located upstream. They are more vertical in the upstream face of the barrages, revealing high connectivity between porous facies in the barrages and tufa beds in pools in the downstream direction. Moreover, it can be observed that in zone 6 (Fig. 1) the upper part of the barrage located downstream is topographically higher than that located upstream (Fig. 8B). This, and onlapping of RB over the upstream barrage, indicates that aggradation could be related with an increasing base level induced by damming. The high sedimentation rate was controlled by fast carbonate precipitation and progressive growth of tufa barrages hindering sediment distribution downstream and forcing aggradation. It is worth mentioning that perpendicular to the river direction GPR-sections over RA facies exhibit a general displacement towards the recent river throughout the Holocene (Fig. 7). In fact, tufas are very rare in the right riverbank of the valley.

The evolution of DV2 and DV3 show a higher development of tufa build-ups during the Pleistocene and the lower middle part of the Holocene. The reduction of these facies and a higher detrital carbonate sedimentation, indicates, as GPR, a progressive fill of a pool or slow flowing area between barrages trough time. The possible sedimentary hiatus in the lower part of the Holocene inferred from $^{230}Th/^{234}U$ datings is proposed to represent the middle part of the Holocene Climate Optimum. With respect the isotopical composition of carbonates from DV2, the regression lines for the three units (Fig. 6) have a different origin, indicating that the water source, could have changed through time (Talbot, 1990), although always being typical of freshwater environments. Non-covariant $\delta^{18}O$-$\delta^{13}C$ values (r=0,03) in Unit A1, and slightly evolved waters, agree with a fluvial system with low influence of evaporation on the isotopic composition (Talbot, 1990) for the Pleistocene. $\delta^{18}O$ variations are considered to reflect changes either in water temperature or in the recharge characteristics (Andrews et al., 2000). $\delta^{18}O$ values for the Pleistocene facies are lower than for the Holocene ones, in agreement with colder Pleistocene temperatures, as in cold regions rain is isotopically depleted in ^{18}O (Craig, 1961). In fact, long term changes in $\delta^{18}O$ in Late Pleistocene fluvial tufa and lake carbonates have been shown to represent changes in the air temperature that control $\delta^{18}O$ of the rainfall (Craig, 1961; 1965; Andrews et al., 1994; 2000; Andrews, 2006; Marshall et al., 2002; Garnett et al., 2004; 2006). Higher values for the Holocene are related to warmer temperatures due to climate amelioration (Huntley and Prentice, 1993), as previously demonstrated from AÑ1.2. Due to the geographical location of the study site and the pollen results, increase $\delta^{18}O$ for the Holocene could be also a consequence of higher influence of the Mediterranean rain, isotopically enriched in ^{18}O (Cruz-San Julián et al., 1992) with respect the oceanic one. General $\delta^{13}C$ decrease during the Holocene is supposed to be related to increase input of isotopically light soil CO_2 as vegetation increased.

Positive $\delta^{13}C$-$\delta^{18}O$ correlation in the Holocene samples suggests a change in the fluvial system with more hydrologically closed areas, especially during the deposition of A3 (r=0.87). The smaller covariance for Unit A2 could be interpreted as been provoked by higher buffering of pool waters due to higher groundwater recharge (Quade et al., 1995; Dunagan and Turner, 2004) during the Holocene onset. Higher covariance in A3 (if compared to A2) is related, in agreement with GPR profiles, with the existence of higher hidrologically closure of pools (Talbot, 1990). This framework fits with the diversifying of riparian vegetation in a dense wetland related to more stable channel banks that has been interpreted from AÑ1.2 core. Higher $\delta^{13}C$ and $\delta^{18}O$ values registered in A2 and A3 represent stages of more water loss of ^{12}C- and ^{16}O-enriched CO_2 due to evaporation (Stuiver, 1975; Talbot, 1990; Talbot and Kelts, 1990). Relatively high $\delta^{13}C$ values in the whole series would reflect the influence of marshy C4-type vegetation and C3 plants growing under water-stressed conditions that tend to have heavier ^{13}C (Ehleringer, 1988).

5.3. Climate *vs* tufa sedimentation

Comparing data from the different proxies analysed and climate a summary can be proposed (Fig. 11). The older tufa deposits analysed in the area would formed probably during the Bølling/Allerød warm interval in the Late Pleistocene. It is very likely that the growth of tufa would stop during the Younger Dryas cold phase, and terrigenous deposits would cover the Jurassic rocks (as in AÑ1.2 area). Increasing temperature (as pointed by $\delta^{18}O$ values) and humidity in the Holocene onset after the previous cold stage, favoured tufa construction again in the whole valley (Holocene Climate Optimum) and a more diversified vegetation. From this moment and till the end of sedimentation in the Dévanos area, which can be related to lowering of the river entrenchment during the colder Iron Age Epoch, the two studied zones reveal similar environmental changes, with a sedimentary interruption and vegetation change related to the colder central part of the Holocene Climate Optimum. Sediments and pollen above this discontinuity do not allow us to perform a palaeoclimate-related interpretation, as increasing human activities could affect the dynamics of the fluvial system. The tufa growth interruption coincides with the Iron Age Epoch and younger deposits are only preserved in AÑ1.2, where more oxidizing conditions developed contemporaneous with increased erosive processes and higher human impact have been inferred during the Roman and Medieval Warm Periods.

6. Conclusions

The multidisciplinary study carried out in the fluvial deposits of the Añamaza river valley (NE Spain) allows the main palaeoenvironmental changes to be recognised and to deduce that distinct subenvironments and proxies registered valuable palaeoenvironmental information. Dating results (^{14}C and $^{230}Th/^{234}U$) reveal high sedimentation rates during the Holocene and three main stratigraphic discontinuities that we correlate with the Younger Dryas, the colder phase in the middle part of the Holocene Climate Optimum and the Iron Age Epoch.

Widespread of tufa was favoured by warm and humid conditions. Some warmer episodes in the Late Pleistocene (Bølling/Allerød) would favour tufa growing, which was very important too during the Holocene Climate Optimum. Progressive reduction in tufa debris is observed in the upper part of the Holocene. Intraclastic tufas reveal tufa build-ups erosion during high-energy runoff episodes, especially during the first part of the Holocene, but also during colder stages when water levels would decrease. Isotopical results suggest cold temperatures and a carbonate fluvial system with low influence of evaporation during the upper part of the Late Pleistocene. Higher temperatures from the Younger Dryas, increasing mediterranean influence, and a change in the fluvial system, with progressively more hydrologically closed areas characterise the Holocene.

Climate also affected considerably vegetation changes. Scarcely vegetated areas and arid conditions are inferred for the Holocene onset. Woodland migration occurred during the postglacial climatic amelioration (with a pioneer tree open woodland and dry grassland), followed by the establishment of a *Pinus*-*Quercus* open temperate and humid forest and sclerophyllous Mediterranean woodland at lower altitudes. Later on, during the Holocene Climate Optimum, wetland (probably mire) areas developed in the channel banks with increasing and diversifying aquatic herbaceous taxa, expansion of wetland vegetation and disappearance of xerophilous and heliophilous taxa. A discontinuity in the middle part of the Holocene Optimum is clearly recognised from pollen record and thereafter a mixed oak forest (with *Corylus, Ulmus, Taxus, Fagus* and *Pinus*) as well as limited human activities (grazing and crop cultivation) are recorded. Moreover, riparian vegetation developed and diversified. During the Roman and Medieval Warm Periods increasing human activities could affect the dynamics of the fluvial system. In this sense, local deforestation associated with grazing activities coincides with the disappearance of tufa, and anthropogenic activities (pasture and cereal cultivation) provoked progressively replacement of dense wetland by marshland vegetation. Towards the end of the sequence, disappearance of arboreal cover favoured terrigenous supplies incoming, clearly reflected also in mineralogy.

Considering the carbonate fluvial system configuration, two radarfacies (RA and RB) have been defined for the main channelled area. RA (reflective and non-homogeneous) corresponds to tufa constructions, and RB (non-reflective and homogeneous) to pool facies. Differences between radarfacies are related to distinct architecture and texture of the detrital beds. Small RA zones inside RB-dominated areas indicate either expansion of the barrages or growing of isolated pockets and repetitive water level changes. Lateral relations between RB and RA reveal differences in connectivity between the distinct elements. An aggrading fluvial system during the Holocene, with pool sediments onlapping barrages, can be related with increasing base level induced by damming due to carbonate precipitation, in agreement with sedimentological and isotopical results.

7. Acknowledgements

Work supported by CGL2009-09165/BTE MCINN-Feder and UZ2014-CIE-04 and UZ2015-CIE-08 Universidad de Zaragoza projects; it is a contribution of the Análisis de Cuencas Sedimentarias Continentales (Stratos) and Geotransfer (UZ-DGA and Social European Fund) research groups.

8. References

Alley, R.B., 2000. The Younger Dryas cold interval as viewed from central Greenland. Quaternary Science Reviews 19, 213-226.

Andreo, B., Martín-Martín, M., Martin Algarra, A., 1999. Hydrochemistry of spring water associated with travertines. Examples of the Sierra de la Alfaguara (Granada, southern Spain). Comptes Rendus de l'Academie des Sciences Paris, Sciences de la Terre et des Planètes 328, 745-750.

Andrews, J.E., 2006. Palaeoclimatic records from stable isotopes in riverine tufas: Synthesis and review. Earth-Science Reviews 75, 85-104.

Andrews, J.E., Brasier, A.T., 2005. Seasonal records of climatic change in annually laminated tufas: short review and future prospects Journal of Quaternary Science 20, 411-421.

Andrews, J.E., Pedley, H.M., Dennis, P.F., 1994. Stable isotope record of palaeoclimate change in a British Holocene tufa. Holocene 4, 349-355.

Andrews, J.E, Riding, R., Dennis, P.F., 1997. The stable isotope record of environmental and climatic signals in modern terrestrial microbial carbonates from Europe. Palaeogeography, Palaeoclimatology, Palaeoecology 129, 171-189.

Andrews, J.E., Pedley, H.M., Dennis, P.F., 2000. Palaeoenvironmental records in Holocene Spanish tufas: a stable isotope approach in search of reliable climatic archives. Sedimentology 47, 961-978.

Annan, A.P., 1992. Ground Penetrating Radar Workshop Notes, Sensors and Software, Ontario, Canada.

Arenas, C., Gutiérrez, F., Osácar, C., Sancho, C., 2000. Sedimentology and geochemistry of fuvio-lacustrine tufa deposits controlled by evaporite solution subsidence in the central Ebro Depression, NE Spain. Sedimentology 47, 883-909.

Arenas, C., Vázquez-Urbez, M., Pardo, G., Sancho, C., 2014. Sedimentology and depositional architecture of tufas deposited in stepped fluvial systems of changing slope: Lessons from the Quaternary Añamaza valley (Iberian Range, Spain). Sedimentology 61, 133-171.

Ascione, A., Iannace, A., Imbriale, P., Santangelo, N., Santo, A., 2014. Tufa and travertines of southern Italy: deep-seated, fault-related CO_2 as the key control in precipitation. Terra Nova 26, 1-13.

Auqué, L.F., Arenas, C., Osácar, C.; Pardo, G., Sancho, C., Vázquez Urbez, M., 2013. Tufa sedimentation in changing hydrological conditions: the River Mesa (Spain). Geologica Acta 11, 85-102.

Baker, P.L., 1991. Response of ground penetrating radar to bounding surfaces and lithofacies variations in sand barrier sequences. Exploration Geophysics 22, 19-22.

Bastida, J., Osacar, M.C., Sancho, C., Muñoz, A., 2013. Environmental changes during the Upper Pleistocene-olocene in Mediterranean NE Spain as recorded by mineralogy and geochemistry of alluvial records. Quaternary International 302, 3-19.

Behre, K.E., 1981. The interpretation of anthropogenic indicators in pollen diagrams. Pollen et Spores 23, 225-245.

Bell, M., Walker, M.J.C., 1992. Late Quaternary environment Change. Physical and Human perspectives. Longman Scientific and Technical. Nueva York.

Bennett, K.D., 1964. http://www.chrono.qub.ac.uk/psimpoll/psimpoll.html

Beug, H.J., 2004. Leitfaden der Pollenbestimmung für Mitteleuropa und angrenzende Gebiete. Verlag Friedrich Pfeil, München.

Bischoff, J.L., Julià, R,; Mor, R., 1988. Uranium-series dating of the Mousterian occupation at Abric Romani, Spain. Nature 332, 68-70.

Blanco Castro, E., Casado González, M.A., Costa Tenorio, M., Escribano Bombín, R., García Antón, M., Génova Fuster, M., Gómez Manzaneque, Á., Gómez Manzaneque, F., Moreno Saiz, J.C., Moría Juaristi, C., Regato Pajares, P., Sainz Ollero, H., 2005. Los bosques ibéricos. Una interpretación geobotánica. 4ª edición. Planeta, Barcelona.

Burjachs F., Jones S.E., Giralt S., Fernández-López de Pablo J., 2016. Lateglacial to Early Holocene recursive aridity events in the SE Mediterranean Iberian Peninsula: The Salines playa lake case study. Quaternary International 403, 187-200.

Camuera, J., Alonso-Zarza, A.M., Rodríguez-Berriguete, A., Meléndez, A., 2015. Variations of fluvial tufa sub-environments in a tectonically active basin, Pleistocene Teruel Basin, NE Spain. Sedimentary Geology 330, 47-58.

Capezzuoli, E., Gandin, A., Sandrelli, F., 2010. Calcareous tufa as indicators of climatic variability: a case study from southern Tuscany (Italy). Geological Society of London Special Publications 336, 263-281.

Capezzuoli, E., Gandin, A., Pedley, M., 2014. Decoding tufa and travertine (fresh water carbonates) in the sedimentary record: The state of the art. Sedimentology 61, 1-21.

Carthew, K. D., Taylor, M. P., Drysdale, R. N., 2003. Are current models of tufa sedimentary environments applicable to tropical systems? A case study from the Gregory River. Sedimentary Geology 162, 199-218.

Carthew, K. D., Taylor, M. P., Drysdale, R. N., 2006. An environmental model of fluvial tufas in the monsoonal tropics, Barkly karst, northern Australia. Geomorphology 73, 78-100.

Chung, F.H., 1974. Quantitative interpretation of X-ray diffraction patterns of mixtures. II. Adiabatic principle of X-ray diffraction analysis of mixtures. Journal of Applied Crystallography 7, 526-531.

Coloma, P., Martínez Gil, F.J., Sánchez Navarro, J.A., 1996. La laguna de Añavieja. Funcionamiento y génesis. Geogaceta 20, 1258–1260.

Colombo, P.M., Lorenzoni, F.C., Grigoletto F., 1983. Pollen Grain Morphology Supports the Taxonomical Discrimination of Mediterranean Oaks (*Quercus*, *Fagaceae*). Plant Systematics and Evolution 141, 273-284.

Cour, P., 1974. Nouvelles techniques de détection des flux et des retombées polliniques: étude de la sédimentation des pollens et des spores à la surface du sol. Pollen et Spores 16, 103-141.

Craig, H., 1957. Isotopic standards for carbon and oxygen and correction factors for mass-spectrometric analysis of carbon dioxide. Geochimica et Cosmochimica Acta 12, 133-149.

Craig, H. 1961. Isotopic variations in meteoric waters. Science 133, 1702-1703.

Craig, H. 1965. Measurement of oxygen isotope paleotemperatures. In: Tongiorgi, E. (Ed.), Stable Isotopes in Oceanographic Studies and Paleotemperatures. Nuclear Geology Laboratory, Pisa, pp. 161-182.

Cruz-San Julián, J., Araguas, L., Rozanski, K., Benavente, J., Cardena, J., Hidalgo, M.C., García-López, S., Martínez-Garrido, J.C, Moral, F., Olia, M., 1992. Sources of precipitation over South-Eastern Spain and groundwater recharge. An isotopic study. Tellus B 44, 226-236.

Dagallier, G., Laitinen, A., Malartre, F., Van Campenhout, I.P.A.M., Veeken, P.C.H., 2000. Ground penetrating radar application in a shallow marine Oxfordian limestone sequence located on the eastern flank of the Paris Basin, NE. France. Sedimentary Geology 130, 149-165.

Davis, B.A.S., 1994. Paleolimnology and Holocene environmental change from endoreic lakes in the Ebro Basin, north-east Spain, Ph.D. Thesis, University of Newcastle-Upon-Tyne, UK.

Davis B.A.S., Stevenson A.C., 2007. The 8.2 ka event and Early-Mid Holocene forests, fires and flooding in the Central Ebro Desert, NE Spain. Quaternary Science Reviews 26, 1695-1712.

Dunagan, S.P., Turner, C.E., 2004. Regional paleohydrologic and paleoclimatic settings of wetland/lacustrine depositional systems in the Morrison Formation (Upper Jurassic), Western Interior, USA. Sedimentary Geology 167, 269-296.

Ehleringer, J. R., 1988. Carbon isotope ratios and physiological processes in aridland plants. In: Rundel, P. W., Ehleringer, J. R., Nagy K.A. (Eds.), Stable Isotopes in Ecological Research. Ecological Studies Series. Springer-Verlag, New York , pp. 41-54.

Faegri K., Iversen J., 1989. Textbook of Pollen Analysis. IV edition. Wiley, Chichester.

Faust, D., Zielhofer, C., Escudero, R.B., del Olmo, F.D., 2004. High-resolution fluvial record of late Holocene geomorphic change in northern Tunisia: climate or human impact?. Quaternary Science Review 23, 1757-1775.

Fenech, K., 2007. Human-induced changes in the environment and landscape of the Maltese Islands from the Neolithic to the 15th century AD. BAR 1682 Archaeopress, Oxford.

Ford, T.D., Pedley, H.M., 1996. A review of tufa and travertine deposits of the world. Earth-Science Reviews 41, 117-175.

García Álvarez, S., García-Amorena, I., Rubiales, J.M., Morla, C., 2009a. The value of leaf cuticle characteristics in the identification and classification of Iberian Mediterranean members of the genus *Pinus*. Botanical Journal of the Linnean Society 161, 436-448.

García Álvarez S., Moría Juaristi C., Solana Gutiérrez J., García-Amorena I., 2009b. Taxonomic differences between *Pinus sylvestris* and *P. uncinata* revealed in the stomata and cuticle characters for use in the study of fossil material. Review of Palaeobotany and Palynology 155, 61-68.

García Antón M., Franco Múgica F., Maldonado Ruiz J., Morla Juaristi C., Sainz Ollero H., 1995. Una secuencia polínica en Quintana Redonda (Soria). Evolución holocena del tapiz vegetal en el Sistema Ibérico septentrional. Anales Jardín Botánico de Madrid 52 (2), 187-195.

García-García, F., Pla-Pueyo, S., Nieto, L. M., Viseras, C., 2014. Sedimentology of geomorphologically controlled Quaternary tufas in a valley in southern Spain. Facies 60, 53-72.

Garnett, E.R., Andrews, J.E., Preece, R.C., Dennis, P.F., 2004. Climatic change recorded by stable isotopes and trace elements in a British Holocene tufa. Journal of Quaternary Sciences 19, 251-262.

Garnett, E.R., Andrews, J.E., Preece, R.C., Dennis, P.F., 2006. Late Flacial and Early Holocene climate and environment from stable isotopes in Welsh tufa. Quaternaire 17, 31-42.

Giessner, K., 1990. Geo-ecological controls of fluvial morphodynamics in the Mediterranean subtropics. Geoökodynamik 11, 17-42.

Gil García M.J., Ruiz Zapata M.B., 2004. Desarrollo de la vegetación durante el Tardiglaciar y el Holoceno en la Sierra de Cameros (La Rioja, España). Implicaciones climáticas y antrópicas. Zubía 22, 237-250.

Gil García M.J., Valiño M.D., Valdeolmillos Rodríguez A., Ruiz Zapata M.B., 2002. Late-glacial and Holocene palaeoclimatic record from Sierra de Cebollera (northern Iberian Range, Spain). Quaternary International 93-94, 13-18.

Giralt, S., Burjachs, F., Roca, J.R., Julià, R., 1999. Late Glacial to Early Holocene environmental adjustment in the Mediterranean semi-arid zone of the Salines playa-lake (Alicante, Spain). Journal of Paleolimnology 21, 449-460.

Golubić, S., 1969. Cyclic and noncyclic mechanisms in the formation of travertine. Verhandlungen der international Vereinigüng für Limnologie 17, 956-961.

Gonfiantini, R., 1984. Report of Advisory Group Meeting on stable isotope reference samples for geochemical and hydrological investigations, International Atomic Energy Agency, Vienna, Austria.

Gordon, A.D., Birks, H.J.B., 1972. Numerical methods in Quaternary palaeoecology. I. Zonation of pollen diagrams. New Phytol 71, 961-979.

Goudie, A.S., Viles, A., Pentecost, H.A., 1993. The late-Holocene tufa decline in Europe. The Holocene 3, 181-186.

Hallstadius, L., 1984. A method for the electrodeposition of actinides. Nuclear Instruments and Methods in Physics Research 223, 266-267.

Hansen, B.C.S., 1995. Conifer stomate analysis as a paleoecological tool: an example from the Hudson Bay Lowlands. Canadian Journal of Botany 73, 244-252.

Henchiri, M, 2014. Quaternary paludal tufas from the Ben Younes spring system, Gafsa, southwestern Tunisia: Interactions between tectonics and climate. Quaternary International 338, 71-87.

Horvatinčić, N., Čalić, R., Geyh, M. A., 2000. Interglacial growth of tufa in Croatia. Quaternary Research 53, 185-195.

Huntley, B., Prentice, I.C., 1993. Holocene vegetation and climates of Europe. In: Wright Jr, H.E., Kutzbach, J.E., Webb III, T., Ruddiman, W.F., Street-Perrott, F.A., Bartlein, P.J. (Eds.), Global Climates since the Last Glacial Maximum. University of Minnesota Press, Mineapolis, pp. 136-168.

Ivanovich, M., Harmon, R.S., 1992. Uranium-Series Disequilibrium: Applications to Earth, Marine, and Environmental Sciences. Oxford University Press, Oxford.

Iriarte-Chiapusso M.J., Muñoz Sobrino C., Gómez-Orellana L., Hernández-Beloqui B., García-Moreiras I., Fernández Rodriguez C., Heiri O., Lotter A.F., Ramil-Rego P., 2016. Reviewing the Lateglacial-Holocene transition in NW Iberia: A palaeoecological approach based on the comparison between dissimilar regions. Quaternary International 403, 211-236.

Jalut, G., Esteban Amat, A., Riera i Mora, S., Fontugne, M., Mook, R., Bonnet, L., Gauquelin, T., 1997. Holocene climatic changes in the western Mediterranean: installation of the Mediterranean climate. Compte Rendus de l'Academie Sciences de Paris, Sciences de la terre et des planètes. Earth and Planetary Sciences 325, 327-334.

Jenkins, R., Snyder, R.L., 1996. Introduction to X-ray Powder Diffractometry, John Wiley & Sons, New York.

Jiménez, P., Agúndez, D., Alía, R., Gil, L., 1999. Genetic Variation in Central and Marginal populations of *Quercus suber* L. Silvae Genetica 48, 278-284.

Kano, A., Tatsuya Kawai, T.; Matsuoka, J., Ihara, T., 2004. High-resolution records of rainfall events from clay bands in tufa. Geology 32, 793-796.

Kano, A., Hagiwara, R., Kawai, T., Hori, M., Matsuoka, J., 2007. Climatic conditions and hydrological change recorded in a high-resolution stable-isotope profile of a recent laminated tufa on a subtropical island, southern Japan. Journal of Sedimentary Research 77, 59-67.

Kruse, S.E., Schneider, J.C., Campagna, D.J., Inman, J.A., Hickey, T.D., 2000. Ground Penetrating radar imaging of cap rock, caliche and carbonate strata. Journal of Applied Geophysics 43, 239-249.

Leira M., Santos L., 2002. An early Holocene short climatic event in the northwest Iberian Peninsula inferred from pollen and diatoms. Quaternary International 93-94, 3-12.

Limondin-Lozouet, N., Nicoud, E., Antoine, P., Auguste, P., Bahain, J.J., Dabkowski, J., Dupéron, J., Dupéron, M., Falguères, Ch., Ghaleb, M., Jolly-Saad, M.C., Mercier, N., 2010. Oldest evidence of Acheulean occupation in the Upper Seine valley (France) from an MIS 11 tufa at La Celle. Quaternary International 223-224, 299–311.

Luzón, A., Pérez, A., Mayayo, M.J., Soria, A.R., Sánchez, J.A., Roc, A.C., 2007. Palaeogeographical changes since 11,000 yr BP in the Gallocanta lacustrine basin. Iberian Range. NE Spain. The Holocene 17, 649-663.

Luzón, M.A., Pérez, A., Borrego, A.G., Mayayo, M.J., Soria, A.R., 2011. Interrelated continental sedimentary environments in the central Iberian Range (Spain): Facies characterization and main palaeoenvironmental changes during the Holocene. Sedimentary Geology 239, 87-103.

Luzón, M.A., Gautjoer, A.; Pérez, A., Mayayo, M.J., Borrego, A.G., Muñoz, A., 2012. Cambios ambientales y su reflejo en la vegetación durante el Holoceno en el sector central de la Cordillera Ibérica (Cuenca del río Añamaza, NE de España). Geotemas.

Marshall, J.D., Jones, R.T., Crowley, S.F., Oldfield, F., Nash, S., Bedford, A., 2002. A high resolution Late-Glacial isotopic record from Hawes Water, Northwest England Climatic oscillations: calibration and comparison of palaeotemperature proxies. Palaeogeography, Palaeoclimatology, Palaeoecology 185, 25-40.

Martín, J.D., 2004. Using XPowder: a software package for powder X-ray diffraction analysis. From www.xpowder.com.

Martín-Algarra, A., Martín-Martín, M., Andreo, B., Julià, R., González-Gómez, C., 2003 Sedimentary patterns in perched spring travertines near Granada (Spain) as indicators of the paleohydrological and paleoclimatological evolution of a karst massif. Sedimentary Geology 161, 217-228.

McBride, J. H., Guthrie, W. S., Faust, D. L., Nelson, S. T., 2012. A structural study of thermal tufas using ground-penetrating radar. Journal of Applied Geophysics 81, 38-47.

McCrea, J.M., 1950. The isotopic composition of carbonates and a paleotemperature scale. The Journal of Chemical Physics 18, 849-857.

Moore, P.D., Webb, J.A., Collinson, M.E., 1991. Pollen analysis. 2nd edition. Blackwell Scientific Publications, Oxford.

Mukherjee, D., Heggy, E., Khan, S.D., 2010. Geoelectrical constraints on radar probing of shallow water-saturated zone within karstified carbonates in semi-arid environments. Journal of Applied Geophysics 70, 181-191.

Neal, A., 2004. Ground-penetrating radar and its use in sedimentology: principles, problems and progress. Earth-Science Reviews 66, 261–330.

Oliva-Urcía, B., Larrasoaña, J.C., Muñoz, A., González, A., Pérez, A., Luzón, A., Román-Berdiel, T., Villalaín, J.J., 2012. La susceptibilidad magnética como marcador paleoambiental en un abanico aluvial del Pleistoceno superior: la cuenca de Añavieja, Cordillera Ibérica (NE España). Geotemas 13, 243-246.

Oliva-Urcía, B., Muñoz, A., Larrasoaña, J.C., Luzón, A., Pérez, A., González, A., Jiang, Z., Liu, Q., Román-Berdiel, T., Villalaín, J.J., (In press). Response of alluvial systems to Late Pleistocene climate changes recorded by environmental magnetism in the Añavieja Basin (Iberian Range, NE Spain). Geologica Acta.

Ordóñez, S., García del Cura, M.A., 1983. Recent and Tertiary fluvial carbonates in Central Spain. In: Collison, J.D., Lewin, J. (Eds.) Modern and ancient fluvial systems. International Association of Sedimentologist Special Publication 6, pp. 485-497.

Ordóñez, S., Martín, J. G., Del Cura, M. G., Pedley, H. M., 2005. Temperate and semi-arid tufas in the Pleistocene to Recent fluvial barrage system in the Mediterranean area: The Ruidera Lakes Natural Park (Central Spain). Geomorphology 69, 332-350.

Ortiz, J. E., Torres, T., Delgado, A., Reyes, E., Díaz-Bautista, A., 2009. A review of the Tagus river tufa deposits (central Spain): age and palaeoenvironmental record. Quaternary Science Reviews 28, 947-963.

Pazzaglia, F., Barchi, M.R., Buratti, N., Cherin, M., Pandolfi, L, Ricci, M., 2013; Pleistocene calcareous tufa from the Ellera basin (Umbria, central Italy) as a key for an integrated paleoenvironmental and tectonic reconstruction. Quaternary International 292, 59-70.

Pedley, H. M., 1990. Classification and environmental models of cool freshwater tufas. Sedimentary Geology 68, 143-154.

Pedley, M., 2009. Tufas and travertines of the Mediterranean region: a testing ground for freshwater carbonate concepts and developments. Sedimentology 56, 221-246.

Pedley, M., Hill, I., 2003. The recognition of barrage and paludal tufa systems by GPR: case studies in the geometry and correlation of Quaternary freshwater carbonates. In: Bristow, C.S., Jol, H.M. (Eds.), Ground penetrating radar in sediments. Geological Society of London Special Publications 211, pp. 207-223.

Pedley, H.M., Andrews, J., Ordoñez, S., García del Cura, M.A., 1996. Does climate control the morphological fabric of freshwater carbonates? A comparative study of Holocene barrage tufas from Spain and Britain . Palaeogeography, Palaeoclimatology, Palaeoecology 121, 239-257.

Pedley, H.M., Hill, I., Denton, P., Brasington, J., 2000. Three-dimensional modelling of a

Holocene tufa system in the Lathkill Valley, north Derbyshire, using ground penetrating radar. Sedimentology 47, 721-737.

Pentecost, A., Viles, H., 2007. A Review and Reassessment of Travertine Classification. Geographie Physique et Quaternaire 48, 305-314.

Peñalba C., 1994. The history of the Holocene vegetation in northern Spain from pollen analysis. Journal of Ecology 82, 815-832.

Peñalba, M.C., Arnold, M., Guiot, J., Duplessy, J.C., de Beaulieu, J.L., 1997. Termination of the Last Glaciation in the Iberian Peninsula inferred from the Pollen sequence of Quintanar de la Sierra. Quaternary Research 48, 205-214.

Pérez, A., Luzón, A., Soria, A.R., Gómez-Borrego, A., Holmes, J., Mayayo, M.J., 2010. El sistema fluvio-lacustre de Añavieja: facies y evolución sedimentaria durante el Holoceno. Cordillera Ibérica. NE de España. Geogaceta 48, 39-42.

Pérez, A., Pueyo-Anchuela, Ó., Luzón, A., Muñoz, A., González, Á., 2012. Aplicación del georradar al estudio de sistemas fluviales tobáceos: los depósitos holocenos de Añavieja-Dévanos (Soria, NE de España), Geogaceta 52, 121-124.

Pérez-Obiol, R., Jalut, G., Julià, R., Pèlachs, A., Iriarte, M.J., Otto, T., Hernández-Beloqui, B., 2011. Mid-Holocene vegetation and climatic history of the Iberian Peninsula. Holocene 21, 75-94.

Pla-Pueyo, S., Viseras, C., Henares, S., Yeste, L.M., Candy, I. (In press). Facies architecture, geochemistry and palaeoenvironmental reconstruction of a barrage tufa reservoir analog (Betic Cordillera, S. Spain). Quaternary International.
Pla-Pueyo, S., Viseras, C., Henares, S., Yeste, L.M., Candy, I. (In press). Facies architecture, geochemistry and palaeoenvironmental reconstruction of a barrage tufa reservoir analog (Betic Cordillera, S. Spain). Quaternary International.
Planchais, N., 1962. Le pollen de quelques chênes du domaine méditerranéen occidental. Pollen et Spores 4 (1), 87-93.

Pueyo-Anchuela, O., Luzón, A., Perez, A., Gil, H. (2016) Ground penetrating radar evaluation of the internal structure of tufa deposits (Dévanos-Añavieja system, NE Spain): an approach to different scales of heterogeneity. Geophysical Journal International 206, 557-573.

Quade, J., Chivas, A.R., McCulloch, M.T., 1995. Strontium and carbon isotope tracers and the origins of soil carbonate in South Australia and Victoria. Palaeogeography, Palaeoclimatology, Palaeoecology 113, 103–117.

Reille, M., 1992. Pollen et spores d'Europe et d'Afrique du Nord. Laboratoire de Botanique historique et Palynologie, Marseille.

Reille, M., 1995. Pollen et spores d'Europe et d'Afrique du Nord. Supplément 1. Laboratoire de Botanique historique et Palynologie, Marseille.

Reille, M., 1998. Pollen et spores d'Europe et d'Afrique du Nord. Supplément 2. Laboratoire de Botanique historique et Palynologie, Marseille.

Reimer., P.J., Baillie, M.G.L., Bard, E., Bayliss, A., Beck, J.W., Blackwell, P.G., Bronk Ramsey, C., Buck, C.E., Burr, G.S., Edwards, R.L., Friedrich, M., Grootes, P.M., Guilderson, T.P., Hajdas, I., Heaton, T.J., Hogg, A.G., Hughen, K.A., Kaiser, K.F., Kromer, B., McCormac, F.G., Manning, S.W., Reimer, R.W., Richards, D.A., Southon, J.R., Talamo, S., Turney, C.S.M., van der Plicht, J., Weyhenmeyer, C.E. 2009. Radiocarbon 51, 1111-1150.

Rohdenburg, H., 1989. Landscape ecology, geomorphology. Catena, Reiskirchen.

Rosenbauer, R.J., 1991. UDATE1: a computer program for the calculation of Uranium-series isotopic ages. Computers & Geosciences 17, 45-75.

Sánchez Goñi M.F., Hannon G.E., 1999. High-altitude vegetational pattern on the Iberian Mountain Chain (north-central Spain) during the Holocene. The Holocene 9, 39-57.

Sancho, C., Peña, J.L., Meléndez, A., 1997. Controls on Holocene and present-day travertine formation in the Guadalaviar River (Iberian Range, NE Spain). Zeitschrift für Geomorphologie 41, 289-307.

Sancho, C., Muñoz, A., Rhodes, E., McDonald, E., Peña, J.L., Benito, G., Longares, L.A., 2008. Morfoestratigrafía y cronología de registros fluviales del Pleistoceno superior en Bardenas Reales de Navarra: implicaciones paleoambientales. Geogaceta 45, 47-50.

Sancho, C., Arenas, C., Vázquez-Urbez, M., Pardo, G., Lozano, M. V., Peña-Monné, J. L., Torres, T., 2015. Climatic implications of the Quaternary fluvial tufa record in the NE Iberian Peninsula over the last 500ka. Quaternary Research 83: 398-414.

Sbeinati, M. R., Meghraoui, M., Suleyman, G., Gomez, F., Grootes, P., Nadeau, M. J., Al-Ghazzi, R., 2010. Timing of earthquake ruptures at the Al Harif Roman aqueduct (Dead Sea fault, Syria) from archaeoseismology and paleoseismology. Geological Society of America Special Papers 471, 243-267.

Schnurrenberger, D., Russell, J., Kelts, K., 2003. Classification of lacustrine sediments based on sedimentary components. Journal of Paleolimnology 29, 141-154.

Schultz, L.G., 1964. Quantitative interpretation of mineralogical composition from X-ray and chemical data for the Pierre Shale. U.S. Geological Survey Professional Paper 391C.

Sobrón García, I., 1985. Factores de la distribución espacial de *Taxus baccata* L. en la Rioja. Zubía 3, 81-117.

Stuiver, M., 1975. Climate versus changes in ^{13}C content of the organic component of lake sediments during the late Quaternary. Quaternary Research 5, 251-262.

Sweeney, C.A., 2004. A key for the identication of stomata of the native conifers of Scandinavia. Review of Palaeobotany and Palynology 128, 281-290.

Talbot, M.R., 1990. A review of the palaeohydrological interpretation of carbon and oxygen isotopic ratios in primary lacustrine carbonates. Chemical Geology 80, 261-279.

Talbot, M.R., Kelts, K., 1990. Paleolimnological signatures from carbon and oxygen isotopic ratios in carbonates from organic carbon rich lacustrine sediments. In: Katz, B.J. (Ed.), Lacustrine Basin exploration: Case Studies and Modern Analogs American Association of Petroleoum Geology Memories 50, 99-112.

Talvitie, N.A., 1972. Electrodeposition of actinides for alpha spectrometric determination. Analytical Chemistry 44, 280-283.

Taylor, D. M., Griffiths, H. I., Pedley, H. M., Prince, I., 1994. Radiocarbon-dated Holocene pollen and ostracod sequences from barrage tufa-dammed fluvial systems in the White Peak, Derbyshire, UK. The Holocene 4, 356-364.

Trautmann, W., 1953. Zur Unterscheidung fossiler Spaltöffnungen der mitteleuropäischen Coniferen. Flora 140, 523-533.

Van Benthem, F., Clarke, G.C.S., Punt, W., 1984. Fagaceae. In: Punt W., Clarke G.C.S. (Eds.), The Northwest European Pollen Flora IV (33). Elsevier, Amsterdam, 87-110.

Vásquez-Méndez, R., Ventura-Ramos, E., Oleschko, K., Hernández-Sandoval, L., Parrot, J.F., Nearing, M.A., 2010. Soil erosion and runoff in different vegetation patches from semiarid Central Mexico. Catena 80, 162-169.

Vaudour, J., 1986. Travertins holocènes et pression anthropique. Mediteranée 57, 168-173.

Vázquez-Urbez, M., Arenas, C., Sancho, C., Osácar, C., Auqué, L., Pardo, G., 2010. Factors controlling present-day tufa dynamics in the Monasterio de Piedra Natural Park (Iberian Range, Spain): depositional environmental settings, sedimentation rates and hydrochemistry. International Journal of Earth Sciences 99, 1027-1049.

Viles, H., Pentecost, A., 2007. Tufa and travertine. In: David J. Nash, D.J., Sue J. McLaren, S.J. (Eds), Geochemical Sediments and Landscapes. Blackwell Publishing. Malden. Pp. 173-199.

Walters Jr, L.J., Caypool, G.G., Choquette, P.W., 1972. Reaction rates and ^{18}O variation for the carbonate-phosphoric acid preparation method. Geochimica et Cosmochimica Acta 36, 129-140.

White, K., Drake, N., Millington, A., Stokes, S., 1996. Constraining the timing of alluvial fan response to Late Quaternary climatic changes, southern Tunisia. Geomorphology 17, 295-304.

Willing, M.J., 1985. The biostratigraphy of Flandrian tufa deposits in the Cotswold and Mendip districts (Unpublised PhD University of Sussex).

Zak, K., Lozek, V., Kadlec, J., Hladiková, J., Cílek, V., 2002. Climate-induced changes in Holocene calcareous tufa formations, Bohemian Karst, Czech Republic. Quaternary International 91, 137-152.

Zamarreño, I., Anadón, P., Utrilla, R., 1997. Sedimentology and isotopic composition of Upper Palaeocene to Eocene non-marine stromatolites, eastern Ebro Basin, NE Spain. Sedimentology 44, 159-176.

Fig. 1. a) Geological setting of the studied area (black rectangle) in the Iberian Range. The situation of the cores drilled (AÑ1.2, DV2 and DV3) and GPR profiles showed in this work is also marked. b) Situation of the areas where GPR survey was developed (dashed square in a).

Fig. 2. Main sedimentological features and units in AÑ1.2 core. Mineralogical percentages are also included. Calibrated ^{14}C datings are indicated in the left side of the log.

Fig 3. Diagram of selected pollen taxa versus depth, Añavieja core AÑ1-2. Dots indicate percentages lower than 0.5%. The thick dotted line is used to represent a possible gap in sedimentation.

Fig. 4. Summary pollen diagram versus depth, Añavieja core AÑ1-2. The thick dotted line is used to represent a possible stop of sedimentation. Ecological groups: steppic plants (*Ephedra*, *Ephedra distachya*-t., *Ephedra fragilis*-t., *Artemisia* and Chenopodiaceae-t.), pioneer trees (*Juniperus*, *Betula* and *Hippophaë rhamnoides*), trees & shrubs (*Abies*, *Cedrus*, *Picea*, *Taxus*, *Acer*, *Hedera*, *Alnus*, *Carpinus betulus*-t., *Carpinus orientalis*-t., *Corylus*, *Sambucus*, *Viburnum*, *Fagus*, deciduous *Quercus*-t., *Juglans*, *Fraxinus excelsior*-t., *Rhamnus*, *Populus*, *Salix*, *Ribes*, *Ulmus* and *Vitis*), Mediterranean plants (*Pistacia*, *Quercus ilex*-t., *Quercus suber*-t., *Fraxinus ornus*, *Ligustrum*, *Olea*, *Phillyrea*, *Celtis* and *Cistus*), cereals (*Hordeum*-t., *Secale*-t. and *Triticum*-t.), anthropogenic indicators (Papaveraceae, *Plantago*, *Plantago lanceolata*-t., *Polygonum*, *Polygonum aviculare*-t., *Rumex*, Urticaceae and *Urtica pilulifera*), other herbaceous plants (Apiaceae, *Hydrocotyle*, *Anthemis*-t., *Aster*-t., *Centaurea*, *Centaurea nigra*-t., *Centaurea scabiosa*-t., *Cirsium*-t., Asteroideae, Cichorioideae, Boraginaceae, Brassicaceae, Campanulaceae, *Cannabis-Humulus*-t., Caryophyllaceae, *Corrigiola*, *Herniaria*, *Helianthemum*, *Convolvulus*, Crassulaceae, *Knautia*, *Scabiosa*-t., Ericaceae, *Euphorbia*, *Mercurialis*, Fabaceae, *Astragalus*-t., *Lotus*-t., *Trifolium*-t., *Vicia*-t., *Fumaria*, Gentianaceae, *Centaurium*-t., *Erodium*, Lamiaceae t. 3, *Teucrium*, Lamiaceae t. 6, Liliaceae, *Asphodelus*, *Linum*, Malvaceae, Onagraceae, *Limonium*-t., Poaceae, Primulaceae, Ranunculaceae, *Helleborus*-t., *Thalictrum*, Rosaceae, *Alchemilla*-t., *Filipendula*, *Potentilla*-t., *Sanguisorba minor*, Rubiaceae, *Thesium*, Saxifragaceae, *Saxifraga aizoon*-t., Scrofulariaceae, *Euphrasia*-t., Solanaceae, Valerianaceae, *Centranthus* and Violaceae), aquatic plants (*Alisma*, *Callitriche*, Cyperaceae, *Cladium*, *Myriophyllum alterniflorum*-t., *Myriophyllum verticillatum*-t., *Hydrocharis morus-ranae*, Lythraceae, *Menyanthes*, *Nymphaea*, *Polygonum amphibium*-t., *Potamogeton*, *Sparganium-Typha*-t. and *Typha latifolia*), algae (*Botryococcus*, *Closterium idiosporum*-t., *Mougeotia*, *Pediastrum*, *Spirogyra*, *Zygnema* and *Filinia*).

Fig. 5. Main sedimentological features and units defined for DV2 and DV3 cores. U/Th datings and isotopical ($\delta^{18}O$ and $\delta^{13}C$) values for DV2 are also included.

Fig 6: $\delta^{18}O$ vs. $\delta^{13}C$ in calcite in DV2 core. Straight lines are regression lines of A1 (r=0.001), A2 (r= 0,1846), and A3 (r= 0,7633).

Fig. 7. GPR profile (100 MHz) performed normal to the expected flow direction. Geometrical changes and accommodation geometries are marked in the plot by arrows, which indicate a

main displacement of the carbonate system towards the East and define an asymmetrical filling of the valley.

Fig. 8. A: GPR profile (50 MHz) carried out along zone 6 (see location in figure 1b), parallel to the expected flow direction. Location of boreholes DV2 and DV3 is showed and the main radarfacies defined (RA and RB) can be observed. B: GPR profile (250 MHz) carried out along zone 6; it is coincident with profile in figure 8A. The contact between RA and RB facies is marked in the plot: net (left side) and progressive (right side). Onlap marked by an arrow.

Fig. 9. Distribution of the radarfacies A and B (RA and RB) along different (TWT-depth intervals) in zone 6 (see fig. 1 for location). Geometrical relationships are described as progressive or net contact. This model was constructed from different parallel and perpendicular GPR profiles.

Fig 10. a) Present-day distribution of *Taxus baccata* in Spain (Blanco Castro et al., 2005). b) Present-day distribution of *Quercus suber* (Blanco Castro et al., 2005). c) Map of the Añavieja area showing isolated small stands of *Taxus* in Peña Isasa (white vertical bars) and *Quercus suber* in Sierra de la Virgen (white horizontal bars) (Sobrón García I., 1985; Jiménez et al., 1999; Blanco Castro et al., 2005).

Fig. 11. Correlation of results and data inferred from the study of AÑ 1.2, DV2 and DV3 logs. The table contains a palaeoenvironmental synthesis of the studied fluvial system (lithological units, pollen zones, mineralogical mean content vertical evolution and $\underline{\delta}^{18}O$ DV2 carbonate isotopical values), as well as correlation with temperatures deduced from GISP2 ice core (Alley, 2000). Non-filled circles in the GISP2 curve show the isotopical values trend inferred in DV2. Note the parallelism with the GISP2 trend that demonstrates a climate-dependent evolution for the carbonate fluvial system. Ages in AÑ1.2 are ^{14}C calibrated ages and in DV2 $^{230}Th/^{234}U$ ages. Ages in italics are based on previously published works (Luzón et al. 2011; 2012); they have been positioning in the age scale in order to date active sedimentation in the area. Discontinuities inferred from stratigraphy, dating and pollen data. The lower one is based on the position of the Pleistocene-Holocene deposits overlying Mesozoic rocks. The middle one, as explained in the text, evinces a net change in pollen data and vegetation. The upper one is based on the non-existence of younger tufa deposits above the present course of the river, being located the recent ones several metres below the dated ones due to the river entrenchment.

Table 1. AMS radiocarbon dates on organic matter. AÑ1.2 core (dated in this work) and the previously dated AÑ1 core (Luzón et al., 2011) have been included. AMS ^{14}C measurements are calibrated using IntCal program by Reimer et al. (2009)

Table 2. U-series radiometric data and derived dates for samples in DV2.

Table 3. Mean mineralogical composition of AÑ1.2 units. Qtz: quartz; Phy: phyllosilicates, CC: calcite, Py: pirite, Gy: gypsum.

Table 4. Description of the Añavieja AÑ1-2 pollen record.

Table 5. Isotopic $\delta^{18}O$ and $\delta^{13}C$ values in DV2 core.

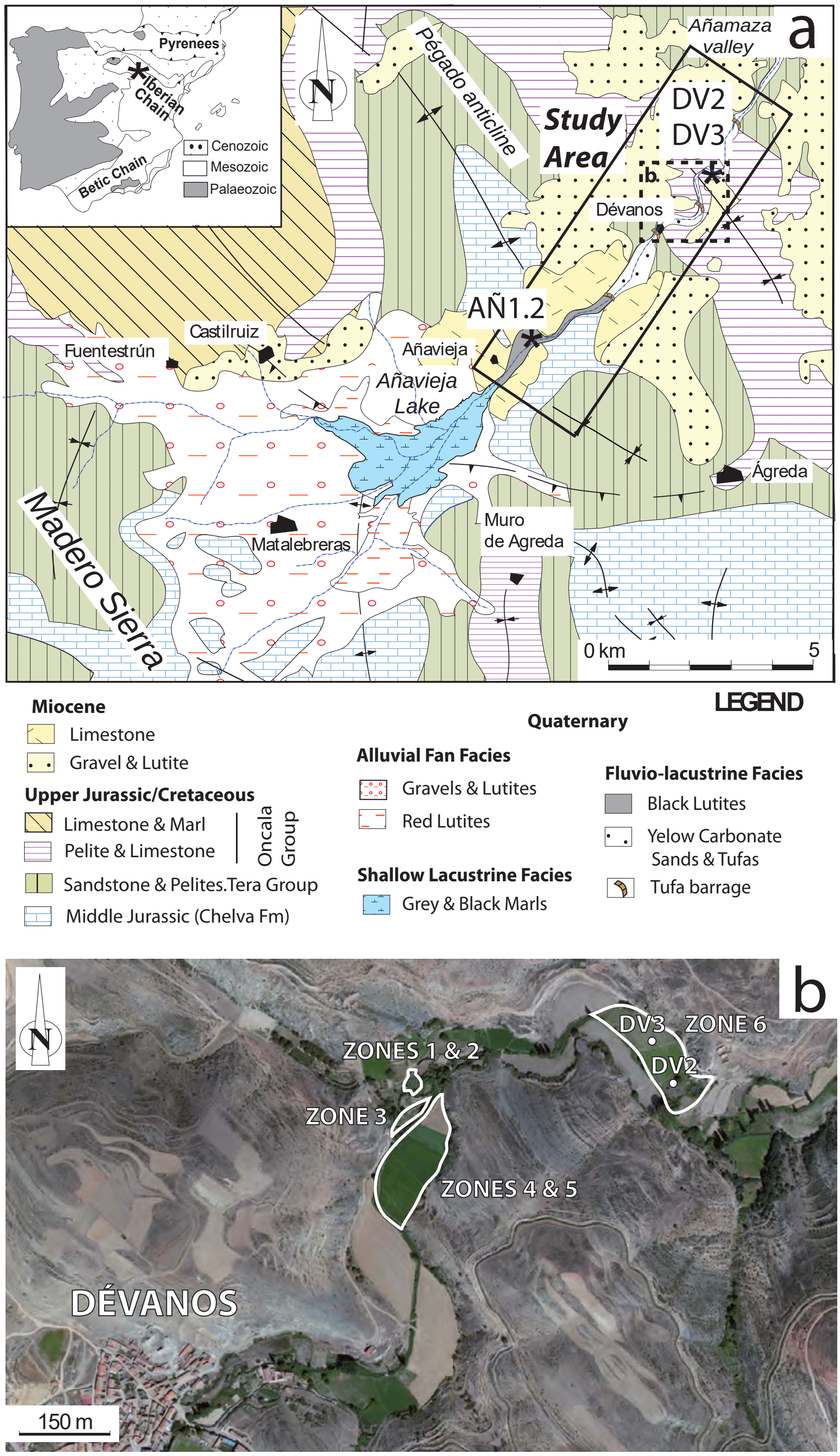
a
Pyrenees
Iberian Chain
Betic Chain
Cenozoic
Mesozoic
Palaeozoic
N
Pégado anticline
Study Area
Añamaza valley
DV2
DV3
b.
Dévanos
AÑ1.2
Castilruiz
Fuentestrún
Añavieja
Añavieja Lake
Ágreda
Muro de Agreda
Matalebreras
Madero Sierra
0 km
5
LEGEND
Miocene
Limestone
Gravel & Lutite
Upper Jurassic/Cretaceous
Limestone & Marl
Pelite & Limestone
Oncala Group
Sandstone & Pelites.Tera Group
Middle Jurassic (Chelva Fm)
Quaternary
Alluvial Fan Facies
Gravels & Lutites
Red Lutites
Shallow Lacustrine Facies
Grey & Black Marls
Fluvio-lacustrine Facies
Black Lutites
Yelow Carbonate Sands & Tufas
Tufa barrage
b
N
ZONES 1 & 2
ZONE 3
ZONES 4 & 5
DV3
ZONE 6
DV2
DÉVANOS
150 m

FIGURE 1.-

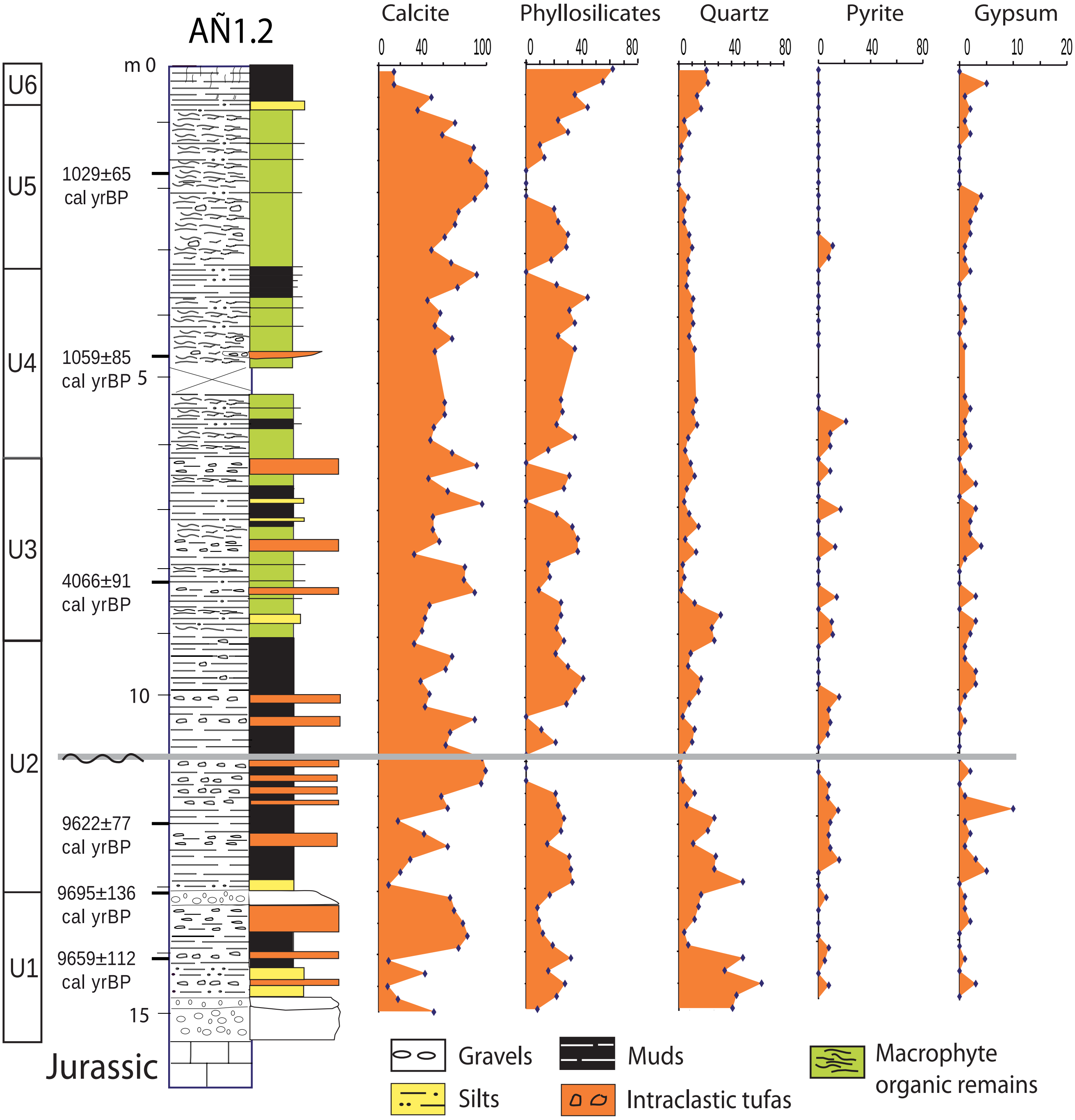
AÑ1.2
m 0
5
10
15
U6
U5
U4
U3
U2
U1
1029±65 cal yrBP
1059±85 cal yrBP
4066±91 cal yrBP
9622±77 cal yrBP
9695±136 cal yrBP
9659±112 cal yrBP
Jurassic
Calcite
Phyllosilicates
Quartz
Pyrite
Gypsum
Gravels
Muds
Macrophyte organic remains
Silts
Intraclastic tufas

FIGURE 2.

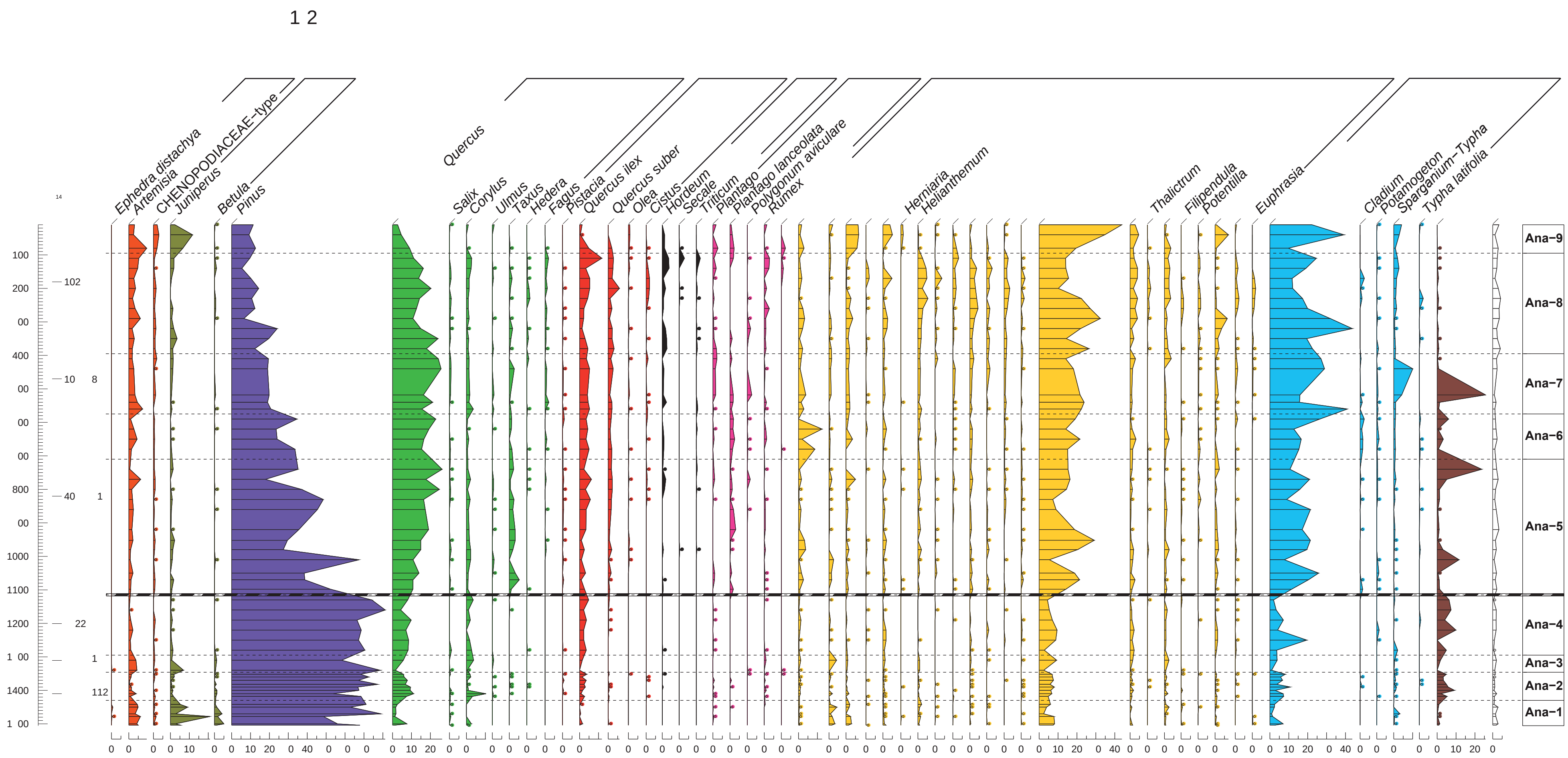
Ephedra distachya
Artemisia
CHENOPODIACEAE-type
Juniperus
Betula
Pinus
Quercus
Salix
Corylus
Ulmus
Taxus
Hedera
Fagus
Pistacia
Quercus ilex
Quercus suber
Olea
Cistus
Hordeum
Secale
Triticum
Plantago
Plantago lanceolata
Polygonum aviculare
Rumex
Herniaria
Helianthemum
Thalictrum
Filipendula
Potentilla
Euphrasia
Cladium
Potamogeton
Sparganium-Typha
Typha latifolia
Ana-9
Ana-8
Ana-7
Ana-6
Ana-5
Ana-4
Ana-3
Ana-2
Ana-1

FIGURE 3

1 2

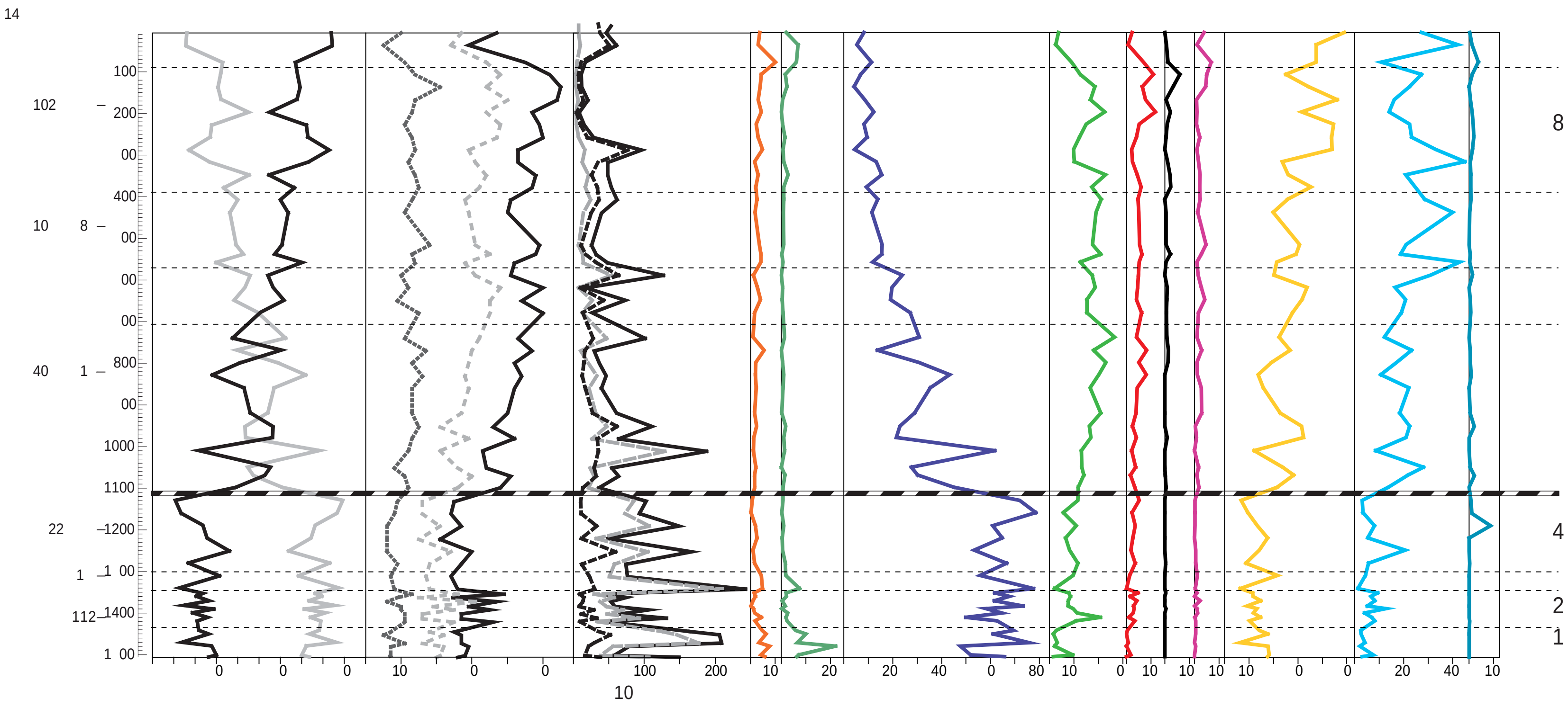

FIGURE 4

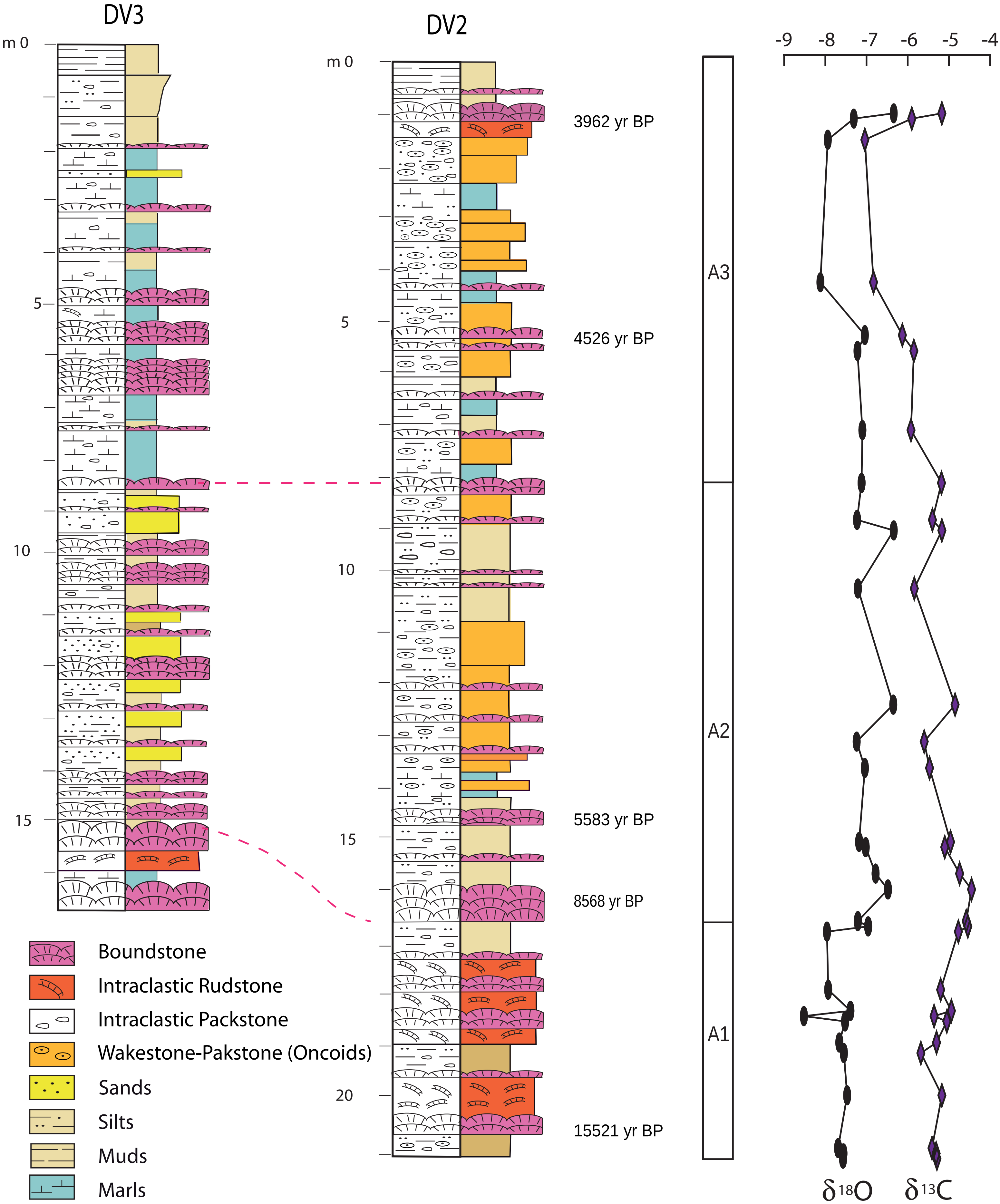

DV3
m 0
5
10
15
DV2
m 0
5
10
15
20
3962 yr BP
4526 yr BP
5583 yr BP
8568 yr BP
15521 yr BP
A3
A2
A1
-9
-8
-7
-6
-5
-4
δ18O
δ13C
Boundstone
Intraclastic Rudstone
Intraclastic Packstone
Wakestone-Pakstone (Oncoids)
Sands
Silts
Muds
Marls

FIGURE 5

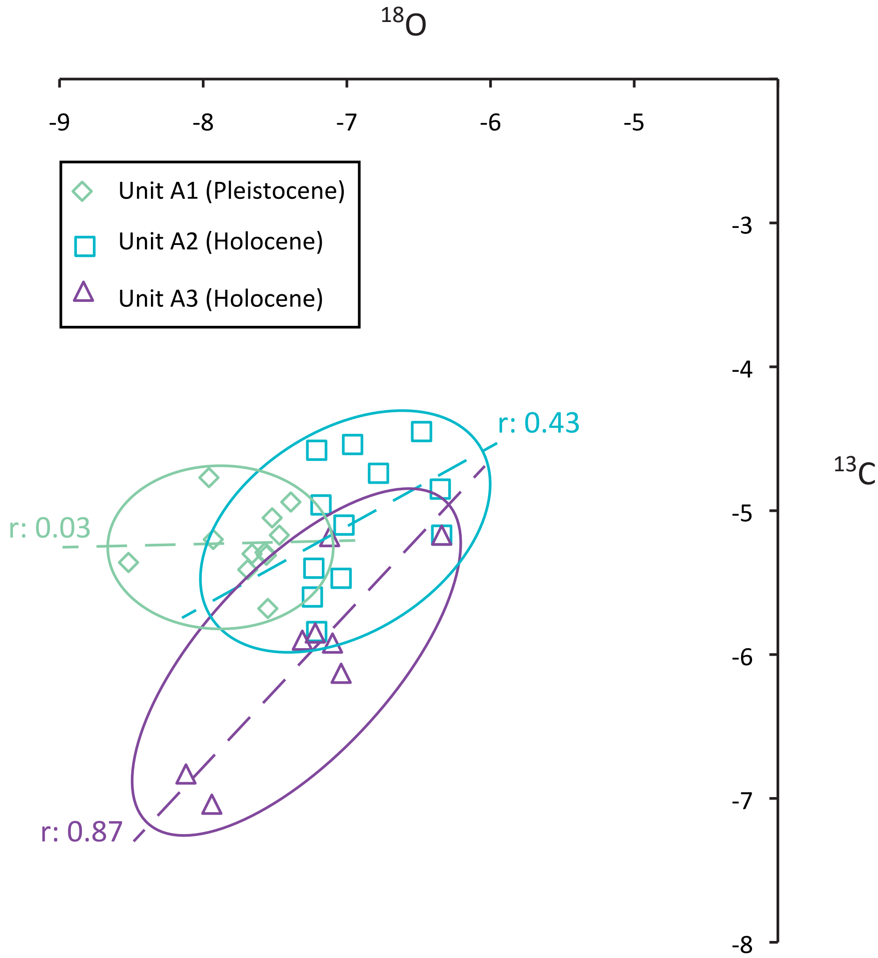

18O
-9
-8
-7
-6
-5
Unit A1 (Pleistocene)
Unit A2 (Holocene)
Unit A3 (Holocene)
-3
-4
-5
-6
-7
-8
13C
r: 0.43
r: 0.03
r: 0.87

FIGURE 6

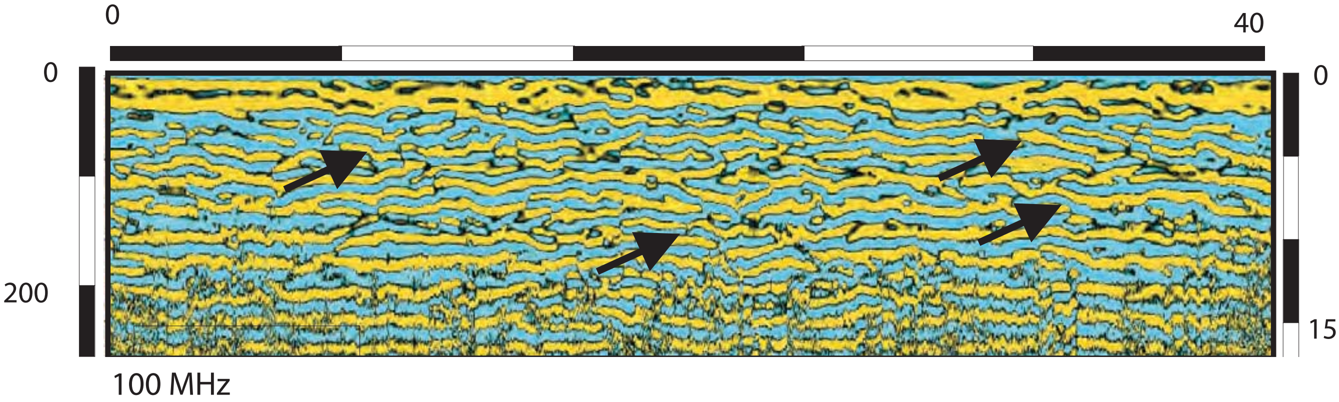

FIGURE 7

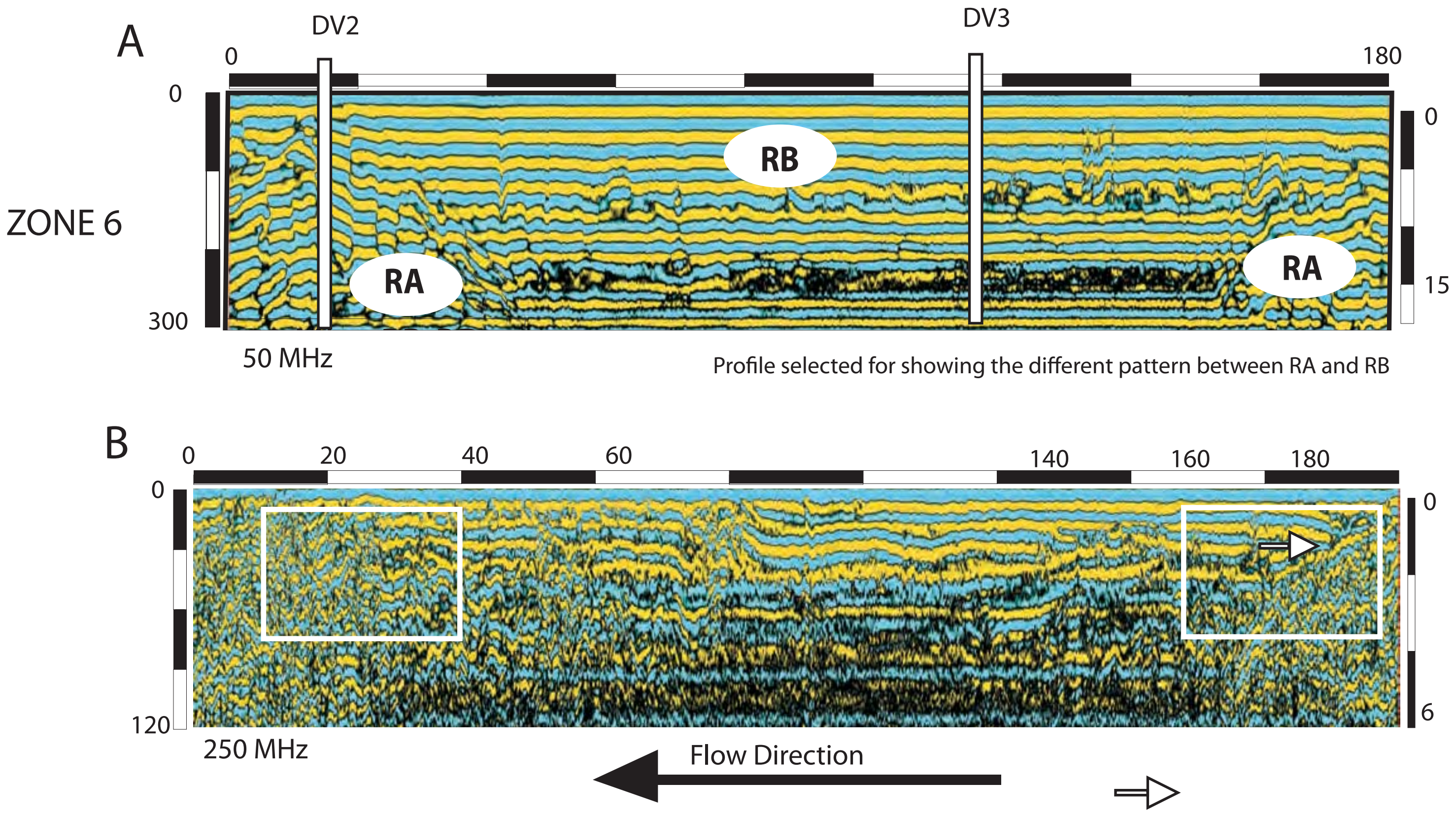
A
DV2
DV3
0
180
0
300
ZONE 6
RB
RA
RA
0
15
50 MHz
Profile selected for showing the different pattern between RA and RB
B
0
20
40
60
140
160
180
0
120
0
6
250 MHz
Flow Direction

FIGURE 8

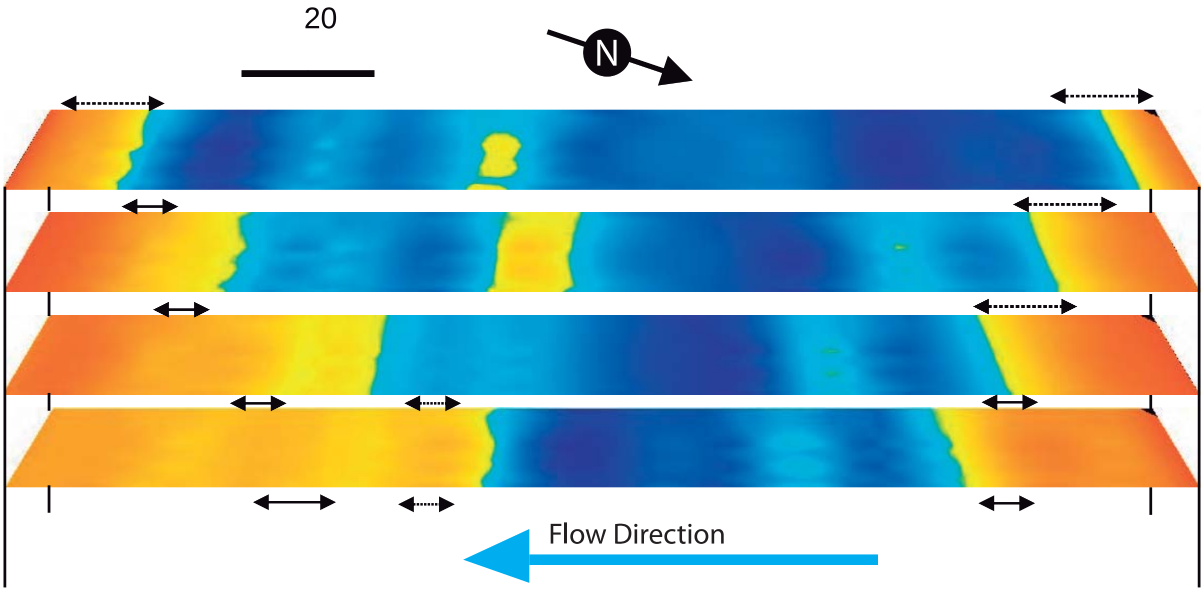

FIGURE 9

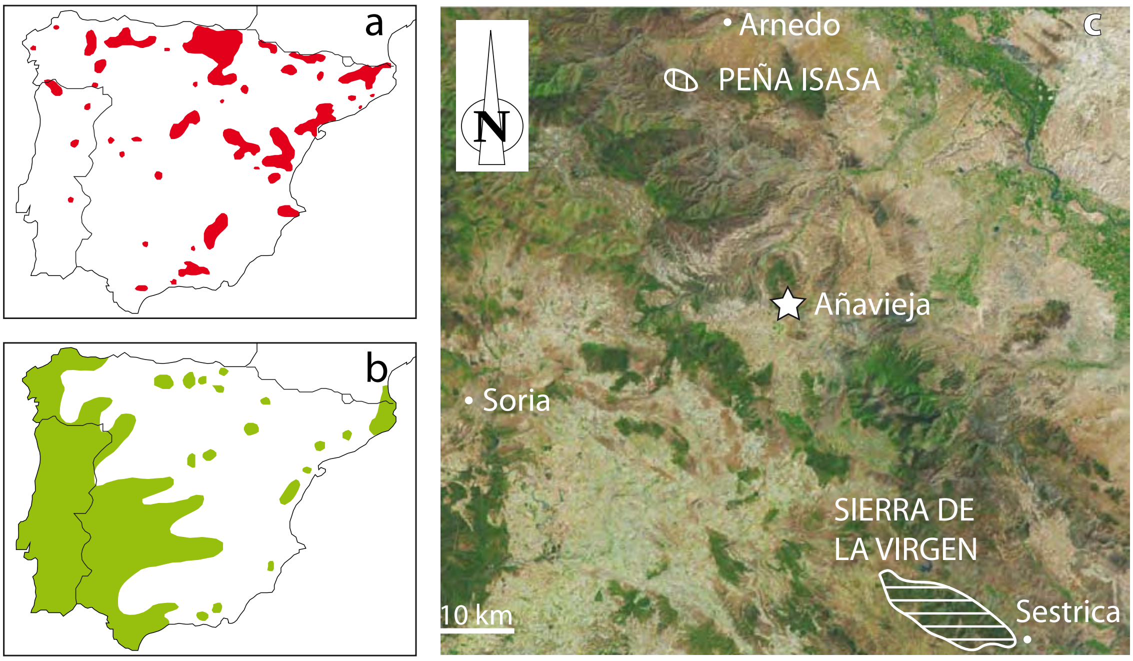
a
b
c
Arnedo
PEÑA ISASA
N
Añavieja
Soria
SIERRA DE
LA VIRGEN
Sestrica
10 km

FIGURE10

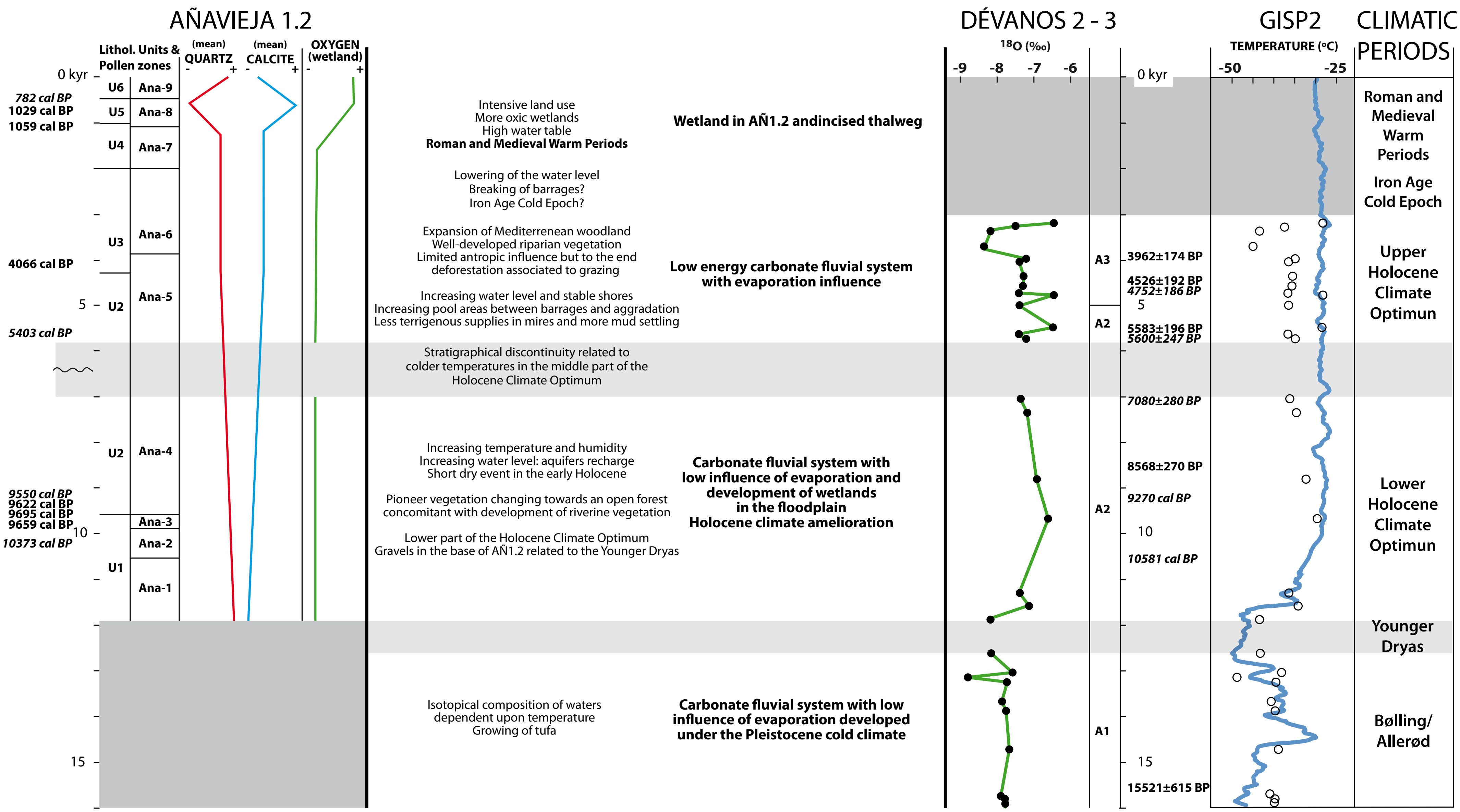

AÑAVIEJA 1.2
Lithol. Units & Pollen zones
(mean) QUARTZ
(mean) CALCITE
OXYGEN (wetland)
0 kyr
782 cal BP
1029 cal BP
1059 cal BP
U6 Ana-9
U5 Ana-8
U4 Ana-7
U3 Ana-6
4066 cal BP
Ana-5
5
U2
5403 cal BP
U2 Ana-4
9550 cal BP
9622 cal BP
9695 cal BP
9659 cal BP
10
10373 cal BP
Ana-3
Ana-2
U1 Ana-1
15
Intensive land use
More oxic wetlands
High water table
Roman and Medieval Warm Periods
Wetland in AÑ1.2 andincised thalweg
Lowering of the water level
Breaking of barrages?
Iron Age Cold Epoch?
Expansion of Mediterrenean woodland
Well-developed riparian vegetation
Limited antropic influence but to the end
deforestation associated to grazing
Low energy carbonate fluvial system with evaporation influence
Increasing water level and stable shores
Increasing pool areas between barrages and aggradation
Less terrigenous supplies in mires and more mud settling
Stratigraphical discontinuity related to
colder temperatures in the middle part of the
Holocene Climate Optimum
Increasing temperature and humidity
Increasing water level: aquifers recharge
Short dry event in the early Holocene
Pioneer vegetation changing towards an open forest
concomitant with development of riverine vegetation
Lower part of the Holocene Climate Optimum
Gravels in the base of AÑ1.2 related to the Younger Dryas
Carbonate fluvial system with
low influence of evaporation and
development of wetlands
in the floodplain
Holocene climate amelioration
Isotopical composition of waters
dependent upon temperature
Growing of tufa
Carbonate fluvial system with low
influence of evaporation developed
under the Pleistocene cold climate
DÉVANOS 2 - 3
18O (‰)
-9 -8 -7 -6
A3
A2
A1
0 kyr
3962±174 BP
4526±192 BP
4752±186 BP
5
5583±196 BP
5600±247 BP
7080±280 BP
8568±270 BP
9270 cal BP
10
10581 cal BP
15
15521±615 BP
GISP2
TEMPERATURE (ºC)
-50 -25
CLIMATIC PERIODS
Roman and Medieval Warm Periods
Iron Age Cold Epoch
Upper Holocene Climate Optimun
Lower Holocene Climate Optimun
Younger Dryas
Bølling/ Allerød

FIGURE 11

AÑ1.2 core.

Depth (m)	Lab. no.	Sample code	δ^{13}C (‰)	^{14}C date yr BP	95.4% (2σ) cal. BP range	Cal. yr BP	Material
1.8	UZ-5866/ETH-40989	AÑ12-18D	-27.3	1135 ± 30	964-1094	1029	Vegetable remains
4.7	UZ-5867/ETH-40990	AÑ12-47D	-26.1	1145 ± 30	973-1144	1059	Vegetable remains
8.2	UZ-5868/ETH-40991	AÑ12-82D	-26.7	3725 ± 35	3974-4157	4066	Vegetable remains
12.0	UZ-5869/ETH-40992	AÑ12-120D	-29.9	8675 ± 35	9544-9699	9622	Vegetable remains
13.1	UZ-5870/ETH-41029	AÑ12-131D	-23.6	8735 ± 35	9558-9831	9695	Vegetable remains
14.1	UZ-5871/ETH-41030	AÑ12-141D	-24.3	8705 ± 35	9547-9771	9659	Vegetable remains

AÑ1 core (Luzón et al., 2011)

Depth (m)	Lab. number	Sample code	δ^{13}C (‰)	^{14}C date yr BP	95.4%(2σ) cal. BP range	Cal. Yr BP	Material
3.8	UZ-5455/ETH-33836	AÑ1-38bD	-22.0	855 ± 50	907-683	782	Vegetable remains
9.7	UZ-5456/ETH-33837	AÑ1-97cD	-15.9	4660 ± 60	5572-5136	5403	Vegetable remains
13.7	UZ-5348/ETH-32047	AÑ1-137aD	-20.7	8555 ± 70	9723-9439	9550	Wood
10.0	UZ-5458/ETH-33839	AÑ1-160bD	-23.1	9200 ± 75	10562-10231	10373	Vegetable remains
0.90	UZ-5679/ETH-37058	AÑ2-9D	-24.7	695 ± 30	680-576	636	Lutites
2.5	UZ-5680/ETH-37059	AÑ2-25D	-23.7	8200 ± 40	9365-9035	9165	Lutites
22.2	UZ-5681/ETH-37404	AÑ2-222D	-21.9	16170 ± 70	19524-19053	19287	Lutites
16.3	UZ-5640/ETH-36372	DV1-163D	-22.5	8280 ± 75	9464-9045	9270	Vegetable remains
20.4	UZ-5641/ETH-36373	DV1-204	-23.3	9365 + 75	10999-10304	10581	Vegetable remains

TABLE 1

Sample	Ref – lab	U-238 ppm	Th-232 ppm	U-234/U-238	Th-230/Th-232	Th-230/U-234	Nominal date (years BP)
DV2-12	4011	0.50	0.14	2.68+/-0.04	1.108+/-0.057	0.04+/-0.00	3962+/-174
DV2-52	3711	0.51	0.12	2.62+/-0.04	1.472+/-0.077	0.04+/-0.00	4526+/-192
DV2-147	4111	0.78	0.04	2.75+/-0.04	9.489+/-0.716	0.05+/-0.00	5583+196/-195
DV2-164	3611	0.79	0.02	2.81+/-0.03	26.441+/-2.743	0.08+/-0.00	8568+/-270
DV2-208(lixi)	3811	0.42	0.28	2.78+/-0.05	1.709+/-0.069	0.13+/-0.01	15521+615/-612

TABLE 2

	AÑ12				
	Qtz	**Phy**	**Cc**	**Py**	**Gy**
U6	18.5	49.0	28.3	0.0	2.7
U5	4.7	16.3	76.2	1.6	1.5
U4	10.0	24.8	57.8	7.8	1.4
U3	10.7	21.5	61.7	4.5	1.6
U2	14.9	21.1	55.2	6.2	1.9
U1	28.7	17.1	49.9	6.8	1.0

TABLE 3

Pollen zone	Depth (cm)	Pollen zone description
Ana-9	95-10	Decrease of diversity (trees and herbs taxa); fall in AP percentages (33-16%), mainly deciduous *Quercus*-t. (9-3%) and absence of all arboreal taxa recorded in the previous zone; stable percentages of *Pinus* (13-9%); increase of *Juniperus* (2-12%); increase of Poaceae (19-44%), Cyperaceae (10-39%), Cichorioideae-t. (6-7%), Brassicaceae (3%), Rubiaceae (1-4%), *Artemisia* (3-9%), Chenopodiaceae-t. (2-3%), *Plantago* (3%) and *Plantago lanceolata*-t. (2%).
Ana-8	395-95	Decrease of *Pinus* (24-5%) and deciduous *Quercus*-t. (24-11%); presence of *Hedera* and *Acer*; notations of *Juglans* and *Carpinus betulus*-t.; at the end, increase of *Quercus ilex*-t. (1-12%), *Quercus suber*-t. (1-6%) and *Cistus* (2%); high diversity of NAP taxa (29-40); increase of Poaceae (10-32%), Cyperaceae (12-44%), Cichorioideae-t. (1-4%), Brassicaceae (0-5%), *Helianthemum* (1-5%), Ericaceae (1-3%), Fabaceae (1-3%), Lamiaceae (1-4%), Rubiaceae (1-6%), *Hordeum*-t. (1-3%), *Triticum*-t. (0-2%) and *Secale*-t. (0-3%).
Ana-7	575-395	Decrease of *Pinus* (21-19%); stable frequencies of deciduous *Quercus*-t., *Corylus* (1-4%), *Fagus* (1-2%), Taxus (1-3%), *Salix* (1%), *Quercus ilex*-t. (4-5%) and *Quercus suber*-t. (1-3%); increase in NAP values, mainly Poaceae (14-24%), Cyperaceae (16-41%) and *Sparganium-Typha*-t. (1-10%); presence of Ericaceae (1%); increase of *Plantago* (2%),*Plantago lanceolata*-t. (2%), *Artemisia* (2-7%) and Chenopodiaceae-t. (2%); decrease of Apiaceae.
Ana-6	710-575	Increase of NAP percentages (51-62%), concentrations (9746-63589 gr/g) and diversity (31-38 taxa); decrease of *Pinus* (35-24%), deciduous *Quercus*-t. (23-15%), *Corylus* (1%) and *Taxus* (1%); stable frequencies of *Quercus ilex*-t. (3-5%) and *Quercus suber*-t. (2%); presence of *Alnus*; increase of Poaceae (14-22%), Cyperaceae (13-26%) and Apiaceae (2-12%).
Ana-5	1115-710	Decrease of *Pinus* (67-18%); increase of deciduous *Quercus*-t. (11-26%), *Corylus* (2%) and *Taxus* (0-5%); presence of *Ulmus*, *Hedera*, *Acer*, *Fagus*, *Salix* and *Populus*; increase of *Quercus ilex*-t. (6%) and *Quercus suber*-t. (2%); presence of *Pistacia*, *Olea*, *Phillyrea*, *Fraxinus ornus*-t. and *Cistus*; increase of Poaceae (5-29%), *Plantago lanceolata*-t. (3%) and *Rumex* (1%); notations of *Hordeum*-t., *Secale*-t. and *Triticum*-t.; increase of Cyperaceae (8-26%.
Ana-4	1295-1115	High values of *Pinus* (66-81%); increase of deciduous *Quercus*-t. (4-10%), *Corylus* (0-4%) and *Quercus ilex*-t. (2-5%); presence of *Quercus suber*-t.; decrease of *Artemisia* (2-0.5%) and *Juniperus* (1-0.5%); absence of *Betula*; increase of Cyperaceae (2-20%) and Monolete spores (0-10%); presence of *Mougeotia* and *Zygnema*.
Ana-3	1346-1295	High values of *Pinus* (58-79%); slight increase of *Juniperus* (1-7%), *Betula* (1%), *Artemisia* (4%), Chenopodiaceae-t. (1%) and Asteroideae-t. (1-4%); presence of *Ephedra*, Cichorioideae-t. and *Helianthemum*; decrease of deciduous *Quercus*-t. (6-1%), *Corylus* (4-0.5%), *Ulmus* and *Quercus ilex*-t.; virtual absence of *Taxus*, *Hedera*, *Pistacia*, *Quercus suber*-t.; decrease of Cyperaceae (4-1%), *Sparganium-Typha*-t. (0.5%) and Monolete spores (2-0%).
Ana-2	1430-1346	High values of *Pinus* (54-77%); increase of deciduous *Quercus*-t. (6-11%) and *Corylus* (0.5-3%); continuous presence of *Viburnum*, *Ulmus*, *Taxus* and *Hedera*; increase of *Quercus ilex*-t. (1-4%); notations of *Pistacia*, *Quercus suber*-t. and *Cistus*; decrease of *Betula, Juniperus, Artemisia* Chenopodiaceae-t., *Helianthemum*, Asteroideae-t. and Cichorioideae-t.; increase of Cyperaceae (3-10%) and Monolete spores (2-9%); presence of *Sparganium-Typha*-t., *Callitriche* and *Nymphaea.*
Ana-1	1504-1430	High values of *Pinus* (>50%); increase of *Juniperus* (20%) and *Betula* (5%); notations of *Hippophae* and *Ephedra*; deciduous *Quercus*-t. (1-8%); dominant herbaceous taxa are Poaceae, *Artemisia* and Chenopodiaceae-t; aquatic plants represented by Cyperaceae and *Sparganium-Typha*-t.

TABLE 4

Sample	Depth (cm)	$\delta^{18}O$	$\delta^{13}C$
1	9	-6,34	-5,17
2	10	-7,31	-5,9
3	14	-7,94	-7,04
4	41	-8,12	-6,83
5	51	-7,04	-6,13
6	54	-7,22	-5,85
7	69	-7,1	-5,92
8	79	-7,12	-5,18
9	86	-7,23	-5,4
10	88	-6,34	-5,17
11	99	-7,21	-5,84
12	121	-6,35	-4,85
13	128	-7,24	-5,6
14	133	-7,04	-5,47
15	147	-7,18	-4,96
16	148	-7,02	-5,1
17	153	-6,78	-4,74
18	156	-6,48	-4,45
19	162	-7,21	-4,58
20	163	-6,96	-4,54
21	164	-7,96	-4,77
22	175	-7,93	-5,2
23	179	-7,39	-4,94
24	180	-8,52	-5,36
25	181	-7,52	-5,05
26	185	-7,66	-5,3
27	187	-7,55	-5,68
28	195	-7,47	-5,17
29	205	-7,69	-5,41
30	206	-7,56	-5,31
31	207	-7,57	-5,29

TABLE 5